From the Department of Clinical Science, Intervention and Technology Division of Radiology
Karolinska Institutet, Stockholm, Sweden

DIFFERENTIATION OF RENAL ONCOCYTOMA FROM RENAL CELL CARCINOMA BY MEANS OF ^{99M}TC-SESTAMIBI SPECT/CT

Antonios Tzortzakakis

Stockholm 2021

Published by Karolinska Institutet.
Printed by Universitetsservice US-AB, 2021

ISBN 978-91-8016-096-4
Cover illustration: Sarantos Stasinakis & Ioannis Koupidis

Differentiation of renal oncocytoma from renal cell carcinoma by means of ^{99m}Tc-Sestamibi SPECT/CT

THESIS FOR DOCTORAL DEGREE (PhD)

By

Antonios Tzortzakakis

The thesis will be defended in public at Karolinska University Hospital Huddinge, 5th of February 2021, 09:00 am

Principal Supervisor:
Professor Rimma Axelsson
Karolinska Institutet
Department of Clinical Science,
Intervention and Technology
Division of Radiology

Co-supervisor(s):
Professor Torkel B. Brismar
Karolinska Institutet
Department of Clinical Science,
Intervention and Technology
Division of Radiology

Maria Holstensson
Karolinska Institutet
Department of Clinical Science,
Intervention and Technology
Division of Radiology

Opponent:
Professor Håkan Geijer
Örebro University
School of Medical Sciences
Division of Radiology

Examination Board:
Professor Lennart Blomqvist
Karolinska Institutet
Department of Molecular Medicine and Surgery
Division Diagnostic Radiology

Associate Professor Johan Stranne
Sahlgrenska Universitet, Göteborg
Department of Urology

Associate Professor Elin Trädgårdh
Lunds Universitet cancercentrum
Department of Nuclear Medicine, Malmö

Τείχη

Χωρίς περίσκεψιν, χωρίς λύπην, χωρίς αιδώ
μεγάλα κι υψηλά τριγύρω μου έκτισαν τείχη.

Και κάθομαι και απελπίζομαι τώρα εδώ.
Άλλο δεν σκέπτομαι: τον νουν μου τρώγει αυτή η τύχη

διότι πράγματα πολλά έξω να κάμω είχον.
Α, όταν έκτιζαν τα τείχη πώς να μην προσέξω.

Αλλά, δεν άκουσα ποτέ κρότον κτιστών ή ήχον.
Ανεπαισθήτως μ' έκλεισαν από τον κόσμον έξω.

Κων/νος Καβάφης, 1896

Murar

Utan förbarmande och utan hänsyn, utan nåd
har man byggt upp omkring mig jättehöga murar.

Här sitter jag och vet i min förtvivlan inte råd,
mitt blinda öde gnager mig i hjärta och i njurar.

Jag hade ju så mycket att beställa utanför.
Ack, varför tog jag inte mig i akt för våldsåtgärden!

Jag hörde inte larmet ens som arbetsstyrkan gör.
Utan att märka något blev jag skild från yttervärlden.

Konstantin Kavafis, 1896 *(översättning: Hjalmar Gullberg)*

To my parents, Kostas and Rena.

Στους γονείς μου. Σας οφείλω τα πάντα.

POPULAR SCIENCE SUMMARY OF THE THESIS

This thesis has proved that a new examination method called ^{99m}Tc-Sestamibi SPECT/CT can help to determine if a kidney tumour is benign or malignant, all without having the patient to go under the knife. Nowadays, the only option to distinguish benign from malignant kidney tumours is either biopsy or operation. To improve the diagnostic accuracy of the above-mentioned examination method, we also propose that kidney tumours showing increased uptake of ^{99m}Tc-Sestamibi should be biopsied and followed by a detailed histological analysis due to their possible benign nature. On the other hand, kidney tumours with decreased uptake of ^{99m}Tc-Sestamibi should be operated since most probably those tumours are malignant. The main benefit of the proposed imaging strategy will be avoiding unnecessary surgery for patients with benign kidney tumours.

ABSTRACT

Purpose: An increasing body of literature indicates the beneficial role of ^{99m}Tc-Sestamibi SPECT/CT in the non-invasive differentiation of renal oncocytoma (RO) from renal cell carcinoma (RCC). This thesis presents a comprehensive approach of ^{99m}Tc-Sestamibi SPECT/CT examination following the implementation of quantitative tools in addition to visual assessment. An additional aim is to explain the differences in ^{99m}Tc-Sestamibi uptake among the different RCC subgroups on histometabolomic grounds.

Methods: 57 radiologically detected kidney tumours from 52 patients were included in the present thesis. Each participant underwent a ^{99m}Tc-Sestamibi SPECT/CT examination before nephrectomy or percutaneous kidney biopsy. Kidney tumours with increased ^{99m}Tc-Sestamibi uptake were classified as positive (Sestamibi positive). In contrast, those with equal or decreased ^{99m}Tc-Sestamibi compared to the ipsilateral non-tumoral kidney parenchyma were classified as negative (Sestamibi negative). Following the visual assessment, quantitative SUV_{mean} and SUV_{max} measurements performed in the examined kidney tumour and the non-tumoral kidney parenchyma that correlated with the histopathological results. Additional immunohistochemical investigation, in situ metabolomics profile characterisation and correlation of mitochondrial content with ^{99m}Tc-Sestamibi SPECT/CT data, were also performed.

Results: Visual assessment of ^{99m}Tc-Sestamibi SPECT/CT examination resulted in a sensitivity of 82% whereas, the quantitative assessment showed a sensitivity of 64% regarding the preoperative characterisation of RO. ^{99m}Tc-Sestamibi SPECT/CT identifies a larger Sestamibi-positive tumour group containing RO, hybrid oncocytic chromophobe tumour (HOCT) and the majority of chromophobe RCC (chRCC). A discriminatory metabolomic signature was identified for Sestamibi positive Birt-Hogg-Dubè-associated HOCT vs other renal oncocytic tumours. Metabolomic differences were also found between Sestamibi positive and negative chRCCs.

Conclusion: Sestamibi positive kidney tumours on SPECT/CT examination are possibly of benign nature. Quantitative assessment with SUV SPECT measurements did not improve the diagnostic performance of ^{99m}Tc-Sestamibi SPECT/CT. Sestamibi negative kidney tumours should be considered for surgery due to their possibly malignant nature. On the other hand, Sestamibi positive kidney tumours could be suited for biopsy and/or follow up according to surveillance protocols.

LIST OF SCIENTIFIC PAPERS

1) **Tzortzakakis A**, Gustafsson O, Karlsson M, Ekström-Ehn L, Ghaffarpour R, Axelsson R. ***Visual evaluation and differentiation of renal oncocytomas from renal cell carcinomas by means of ^{99m}Tc-Sestamibi SPECT/CT***. EJNMMI Res. EJNMMI Research; 2017;7.

2) **Tzortzakakis A**, Holstensson M, Hagel E, Karlsson M, Axelsson R. ***Intra- and Interobserver Agreement of SUV SPECT Quantitative SPECT/CT Processing Software, Applied in Clinical Settings for Patients with Solid Renal Tumors.*** J Nucl Med Technol. 2019;47:258–62.

3) Papathomas T *, **Tzortzakakis A** *, Sun N *, Erlmeier F, Bozoky B, Kokaraki G, et al. ***In Situ Metabolomics Expands the Spectrum of Renal Tumours Positive on ^{99m}Tc-Sestamibi Single Photon Emission Computed Tomography / Computed Tomography Examination***. Eur Urol Open Sci. European Association of Urology.; 2020;22:88–96

4) **Antonios Tzortzakakis**, Thomas Papathomas, Ove Gustafsson, Stefan Gabrielson, Kiril Trpkov, Linnea Ekström-Ehn, Bela Bozoky, Wanzhong Wang, Alexandros Arvanitis, Maria Holstensson, Mattias Karlsson, Georgia Kokaraki, Eva Hagel, Rimma Axelsson. ***Differentiation of renal oncocytoma from renal cell carcinoma by means of ^{99m}Tc-Sestamibi SPECT/CT.*** (manuscript)

CONTENTS

LIST OF ABBREVIATIONS

RO	Renal Oncocytoma
SPECT/CT	Single Photon Emission Computed Tomography/Computed Tomography
MIDOR	Molecular Imaging in Differentiation of Renal Oncocytoma from Renal Cell Carcinoma
RCC	Renal Cell Carcinoma
CT	Computed Tomography
CECT	Contrast-Enhanced Computed Tomography
MRI	Magnetic Resonance Imaging
ADC	Apparent Diffusion Coefficient
US	Ultrasound
CEUS	Contrast-Enhanced Ultrasound
PET/CT	Positron Emission Tomography/Computed Tomography
FDG	Fluorodeoxyglucose
SPECT	Single Photon Emission Computed Tomography
ccRCC	Clear Cell Renal Cell Carcinoma
pRCC	Papillary Renal Cell Carcinoma
chRCC	Chromophobe Renal Cell Carcinoma
ccpRCC	Clear Cell Papillary Renal Cell Carcinoma
HOCT	Hybrid Oncocytic Chromophobe Renal Cell Carcinoma
LOT	Low Grade Oncocytic Renal Tumour
AML	Angiomyolipoma
WHO	World Health Organization
ROI	Region of Interest
VOI	Volume of Interest
ICC	Intraclass Correlation Coefficient
SUV	Standard Uptake Value
HE	Haematoxylin & Eosin
IHC	Immunohistochemistry
TMA	Tissue Microarray Analysis
SDHB	Succinate DeHydrogenase complex subunit B
ROC	Receiver Operating Characteristic
BHD	Birt-Hogg-Dubè

1 INTRODUCTION AND LITERATURE REVIEW

1.1 Epidemiology of renal neoplasia

Kidney cancer accounts for almost 5% of all the new cancer cases diagnosed annually [1]. The most common histological type of kidney cancer arising from renal tubular epithelium with a prevalence of 75% among all primary kidney cancers is the renal cell carcinoma (RCC) [2]. RCC contributes to 5% of all cancers in the male, and 3% of all cancers in the female population [3] with hereditary predisposition accounting for approximately 5% of all RCC cases [4]. Despite the gradual increase of RCC incidence, stabilisation of the mortality rates has been observed mainly in developed countries but not in developing countries [5]. The incidence of RCC may vary universally, but the regions of the highest rates are observed in the Czech Republic, Eastern-North Europe, Australia, and North America [3,6]. According to the latest data reports (2018) from the World Health Organization (WHO), RCC ranks in the 13th position of cancer-related deaths worldwide [3].

1.2 RCC subtypes

The three main RCC subcategories include *clear cell RCC (ccRCC), papillary RCC (pRCC) types 1-2 and chromophobe RCC (chRCC), accounting for 70%-80%, 14%–17% and 4%–8% of cases respectively* [7]. The metastatic rate of the RCC subtypes above is highest for ccRCC (8,7%) followed by pRCC (5,5%) and then chRCC (2,9%) [8]. Other malignant tumours of the kidney apart from RCC, are transitional cell carcinoma (urothelial carcinoma of the renal pelvis) and nephroblastoma in children (Wilms tumour) [2,7].

The dynamic nature of scientific advances leads to a continuous re-evaluation of RCC, as reflected in the recent edition (2016) of the WHO classification of urogenital neoplasia [9]. The latest re-examination of RCC from the WHO led to the recognition of 12 RCC subtypes and the emerge of other RCC entities [10]. A worth mentioned example of a newly recognised separate RCC entity is clear cell papillary RCC, a tumour of good prognosis previously described in patients of chronic kidney disease [9,10]. Hybrid chromophobe oncocytic tumour (HOCT) which is still a subtype of chRCC on the most recent WHO classification, emerges nowadays as a distinct clinicopathological entity on molecular grounds [11]. Another example of an emerging renal tumour seeking recognition as a separate entity is low grade oncocytic renal tumour (LOT), which is a tumour of overlapping morphology with renal oncocytoma (RO) and eosinophilic chRCC [12].

1.3 Benign renal neoplasia

RO derives from the distal tubular renal epithelium [13], exhibits eosinophilia due to its abundance in mitochondria [14] and constitutes almost 5% of all renal epithelial neoplasms, data based on surgical specimens [15,16]. As the second benign renal tumour category after angiomyolipoma (AML), RO was considered a malignant entity for almost 35 years since its first description in the early ’40s [17]. Both RO and AML contribute to 10% of unnecessary nephrectomies since they share common imaging characteristics with RCC [16,18] (**Fig**.1). Simple renal cysts are also benign while complicated renal cysts classified according to Bosniak can be further characterised as cysts of low or high malignant potential [19].

Figure 1. Two different patients, two different renal tumours (arrows) incidentally discovered. Contrast-enhanced axial CT scans of the abdomen exhibiting small tumours on the right kidney. Both tumours share common imaging characteristics which makes an accurate preoperative diagnosis difficult. The tumour on the left (a) turned out to be RCC of clear cell subtype while the tumour on the right (b) was postoperatively diagnosed as a benign RO. *(Karolinska University Hospital Huddinge, MIDOR study)*

1.4 Symptoms of renal neoplasia

The widespread use of different abdominal imaging techniques leads to increased incidental detection of renal tumours. The old classic triad of symptoms, namely flank pain, macrohematuria and a palpable mass in the abdomen indicates nowadays a relatively advanced disease often followed by paraneoplastic symptoms [20].

1.5 Imaging of renal neoplasia

Since no reliable serum or urine biomarkers for kidney cancer exist despite recent advances [21,22], imaging plays a unique role in its detection and characterisation [23]. Ultrasound (US), contrast-enhanced ultrasound (CEUS), contrast-enhanced computed tomography (CECT), perfusion computed tomography (CTp), magnetic resonance imaging (MRI), positron emission tomography/computed tomography (PET/CT) and recently single-photon computed tomography/computed tomography (SPECT/CT) are preoperative diagnostic tools used to detect, characterise and stage renal neoplasia [18,24]. The accurate non-invasive characterisation of solid renal tumours still raises diagnostic difficulties due to shared, non-pathognomonic imaging characteristics between benign and malignant counterparts [25].

1.5.1 CT and MRI

CT and MRI can easily detect and characterise a fat-rich AML, but accurate diagnosis can be challenging when fat-poor or fat-invisible AML are encountered [26]. Similar diagnostic challenges set the absence or presence of a stellate scar in a solid renal tumour since it is

found in only up to 33% of RO [27]. At the same time, central scars (**Fig**.2) and intravenous contrast uptake with subsequent washout seen on a multiphase CECT (**Fig**.3) are characteristics not only of RO but also of RCC [28].

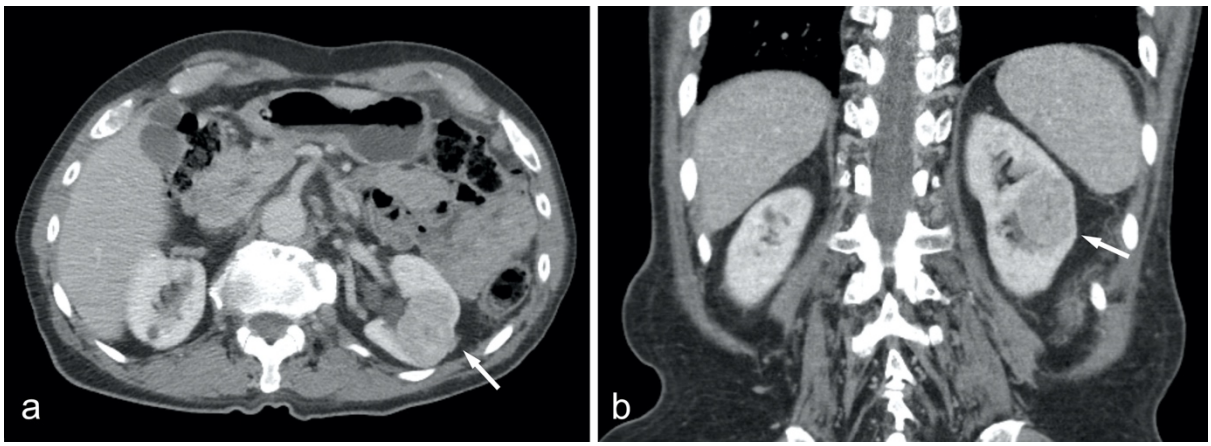

Figure 2: Contrast-enhanced axial (a) and coronal (b) CT plans in the nephrographic phase with a renal oncocytoma on the left kidney exhibiting a subtle central scar. Only 1/3 of renal oncocytomas display central scar, which makes a definite diagnosis difficult since RCC can also show central scar or central necrosis. *(Karolinska University Hospital Huddinge, MIDOR study)*

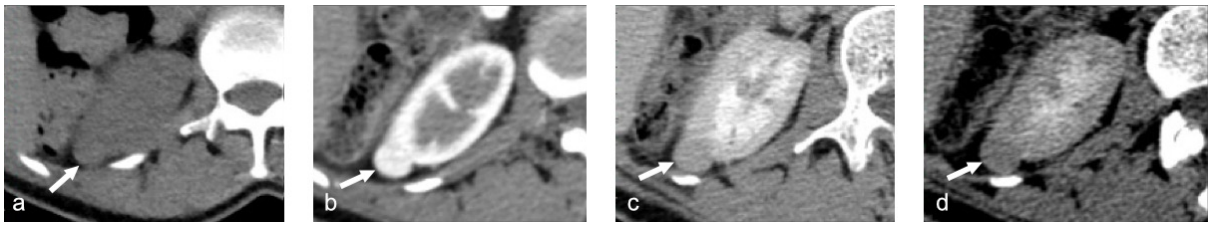

Figure 3: Multiphasic contrast-enhanced axial CT scan of the abdomen exhibiting a small renal oncocytoma on the right kidney. Renal tumour of solid character on the native phase (a) shows contrast uptake (b) on the corticomedullary phase with subsequent washout (c, d) on later nephrographic and excretory phases. Contrast uptake and washout is common imaging characteristic for renal oncocytomas and RCCs. *(Karolinska University Hospital Huddinge, MIDOR study)*

Advances in radiomics using texture analysis on unenhanced or CECT images report promising results concerning the detection of fat-poor AML, the characterisation of RCC subtypes and even the differentiation of RO from chRCC [29–31]. Concerning the value of MRI in imaging renal neoplasia (**Fig**.4), a recent meta-analysis from Tordjman et al. *stands out that apparent diffusion coefficient (ADC) values measured on solid tumour components can differentiate ccRCC from other tumour types exhibiting sensitivity and specificity of 80% and 78% respectively* [32].

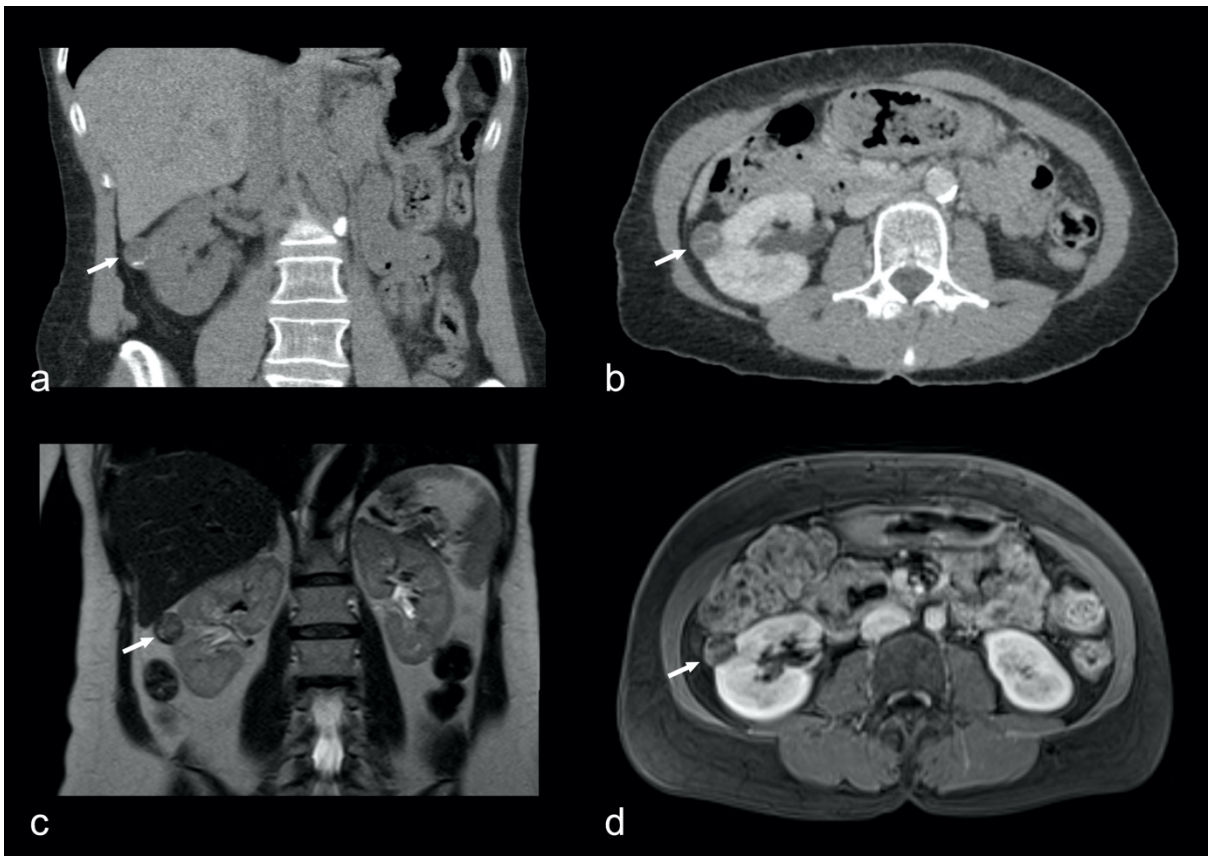

Figure 4: RCC of papillary subtype (arrow) with small calcifications (a) on the native coronal CT scan. The nephrographic phase reveals enhancement of septa (b, d) on the axial CT scan and the T1 weighted MRI axial MRI sequence, respectively. T2 weighted coronal MRI sequence of the upper abdomen (c) in the same patient reveals the non-cystic nature of the renal tumour. *(Karolinska University Hospital Huddinge, MIDOR study)*

1.5.2 CEUS and FDG PET/CT

Conventional US followed by CEUS can successfully differentiate cystic from solid tumour components as well as the presence of renal pseudotumor since the latter follows the same contrast uptake pattern as renal parenchyma. Still, its usage in solid renal tumour differentiation is limited [33] (**Fig**.5). The use of PET/CT having 18F-fluorodeoxyglucose (FDG) as a radiotracer in the recognition and characterisation of renal neoplasia is also limited mainly due to the FDG excretion from the kidney that results in a high background activity within this organ [34,35]. Furthermore, other innovative radiotracers did not succeed in improving the performance of PET/CT in renal cancer imaging [36].

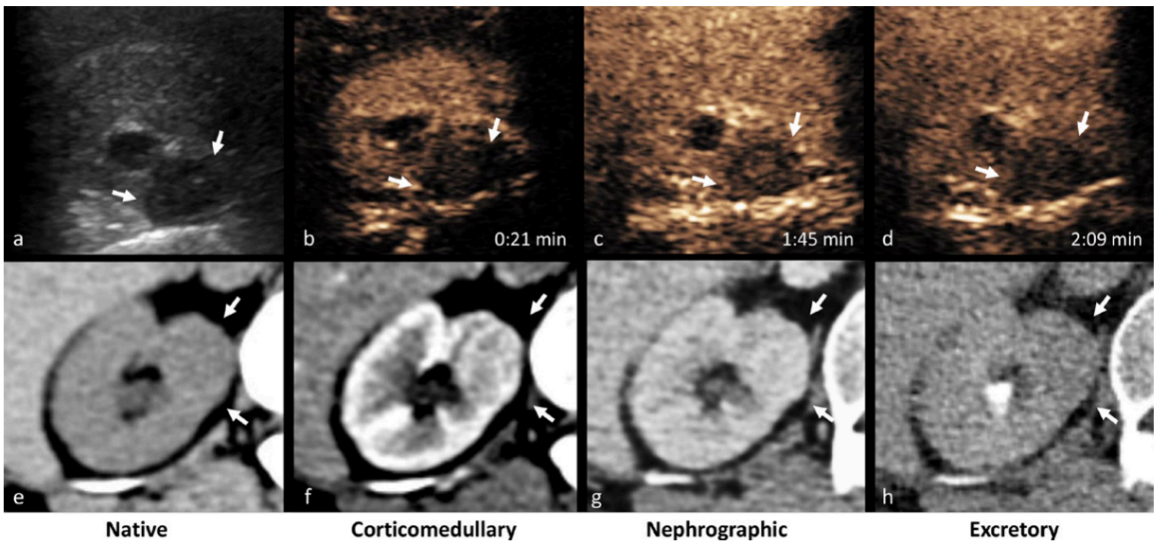

Figure 5: (*a) Grey-scale ultrasonography shows a hypoechoic cortical lesion in the medial aspect of the right kidney. CEUS obtained during the cortical (b) and parenchymal (c,d) phase reveals slow enhancement of the lesion which remains hypoenhancing to surrounding normal renal parenchyma. The lesion has the same attenuation as the adjacent renal parenchyma on unenhanced CT (e) and displays progressive enhancement on corticomedullary(f) and nephrographic(g) phase.* (The above-described kidney tumour turned out to be a HOCT.)

(Figure and Figure legend courtesy of BJR|case reports: Georgios Kalarakis, Katharina Brehmer, Anders Svensson, Rimma Axelsson, Torkel B Brismar, Antonios Tzortzakakis. Combining contrast-enhanced ultrasound, CT perfusion and 99^{m}Tc-Sestamibi SPECT/CT to guide diagnosis in a case of solid renal tumour. BJR|case reports. September 2020)

1.5.3 CTp

The principle of kidney CTp technique is based on the depiction of renal tumour perfusion and its vascular permeability with the acquisition of multiple contrast-enhanced CT scans [37]. CTp parameters *(blood volume: BV, blood flow: BF, permeability surface: PS and mean transit time: MTT)* for the non-tumoral renal cortex and the solid renal tumour are evaluated [38–42]. Differences in perfusion parameters between non-tumoral renal cortex and solid renal lesions have been reported in RCC and among the different RCC categories (**Fig**.6a-f). On the contrary, no differences detected in any of the CTp parameters between RO and non-tumoral renal cortex. To exemplify, Mazzei et al. reported that *"the accuracy, sensitivity, and specificity to predict RCC were 95.92%, 100%, and 66.7%, respectively, for CTp whereas they were 89.80%, 93.35%, and 50%, respectively, for multiphasic CT"* [38]. One of the main limitations of the CTp is the high radiation dose to the patient that restricts the clinical experience on this examination technique despite the low intravenous contrast dose given. As a result, this examination method lacks standardisation, external validation and few published data exist in this specific field of oncologic research imaging.

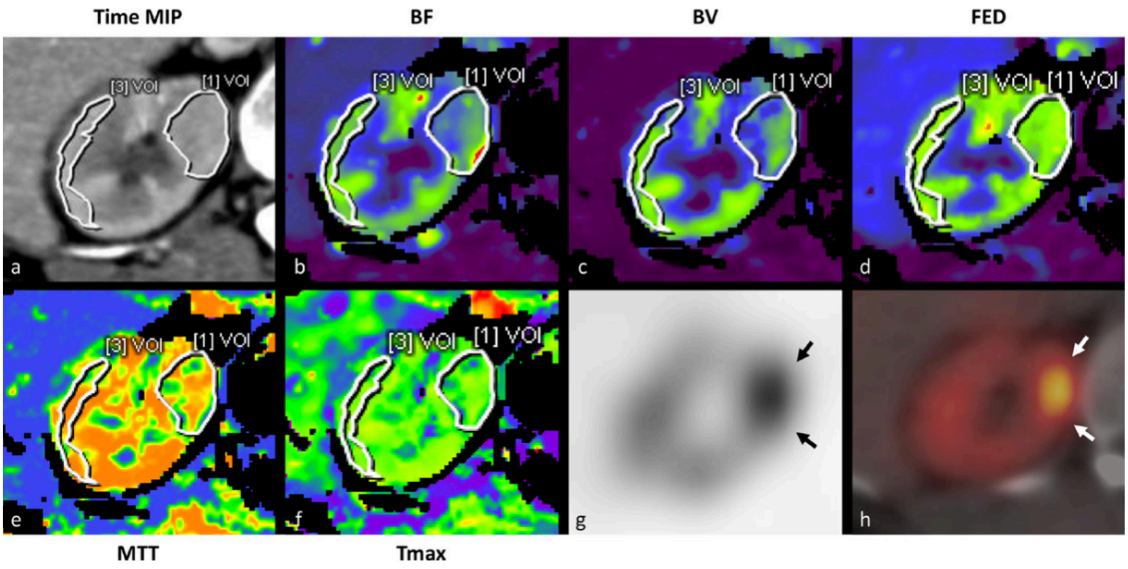

Figure 6: *(a-f) A VOI including the suspect lesion (1) and part of the renal cortex (3) was manually defined in order to calculate the tissue attenuation curve and mean perfusion values. The lesion exhibited lower BF and BV than the renal cortex. On ^{99m}Tc-Sestamibi SPECT/CT (g-h), the lesion demonstrated clear focal uptake relative to surrounding renal parenchyma, indicating its possible benign character.*

MIP; Maximum Intensity Projection, BF; Blood Flow, BV; Blood Volume, MTT; Meant Transit Time, TTP; Time to Peak, Tmax; Time to Maximum; FEP; flow extraction product, VOI; Volume of Interest

(Figure and Figure legend courtesy of BJR|case reports: Georgios Kalarakis, Katharina Brehmer, Anders Svensson, Rimma Axelsson, Torkel B Brismar, Antonios Tzortzakakis. Combining contrast-enhanced ultrasound, CT perfusion and ^{99m}Tc-Sestamibi SPECT/CT to guide diagnosis in a case of solid renal tumour. BJR|case reports. September 2020)

1.5.4 ^{99m}Tc-Sestamibi SPECT/CT

An increasing number of publications indicates the beneficial role of SPECT/CT in the differentiation of RO from RCC using ^{99m}Tc-Sestamibi as a radiotracer. Two recent reviews summarise the relevant published studies that reveal how ^{99m}Tc-Sestamibi uptake from a solid renal tumour indicates its possible benign nature (**Fig**.6g-h) and suggest modern algorithms for the management of ^{99m}Tc-Sestamibi positive (Sestamibi positive) renal tumours [43,44]. The mechanism of ^{99m}Tc-Sestamibi uptake is based on radiotracer's sequestration in the mitochondria of living cells. The last-mentioned property of ^{99m}Tc-Sestamibi is used in oncological research imaging for tracing tumours containing an increased number of mitochondria such as RO and HOCT (**Fig**.7,8) [45]. Scintigraphy efforts have been reported since 1996 when Gormley et al. concluded that *^{99m}Tc-Sestamibi imaging could play a role as a non-invasive method in RO diagnosis* [46]. In this context, Rowe et al. supported the added value of ^{99m}Tc-Sestamibi SPECT/CT in the differential of benign RO from malignant RCC [47]. The hypothesis that RO shows uptake of ^{99m}Tc-Sestamibi on a SPECT/CT examination was verified after demonstrating that a relative ^{99m}Tc-Sestamibi uptake ratio of 0.6 correctly identifies RO and HOCT versus other renal tumours with a sensitivity of 87.5% and a specificity of 95.2% [48]. The relative ^{99m}Tc-Sestamibi uptake ratio measuring the uptake in

the renal tumour and the ipsilateral non-tumoral renal parenchyma could not be correctly assessed on a scintigraphy image before the introduction of SPECT/CT cameras [49]. Advances in software with modern algorithms for image reconstruction accompanied by sophisticated compensation techniques for correction of photon attenuation and scattering have made quantitative SPECT possible like quantitative PET [50]. The aforementioned sensitivity and specificity values were extracted after classifying RO and HOCT as tumours of benign character since both tumour categories showed ^{99m}Tc-Sestamibi uptake and no aggressive behaviour has been documented for HOCT [51] (**Fig**.9). It is noteworthy though that the official WHO classification of renal neoplasia still considers HOCT as a malign entity, namely a subtype of chRCC [11]. Of note is also the fact that 50% of the examined chRCC, which are tumours of indolent clinical course, exhibited ^{99m}Tc-Sestamibi uptake [48].

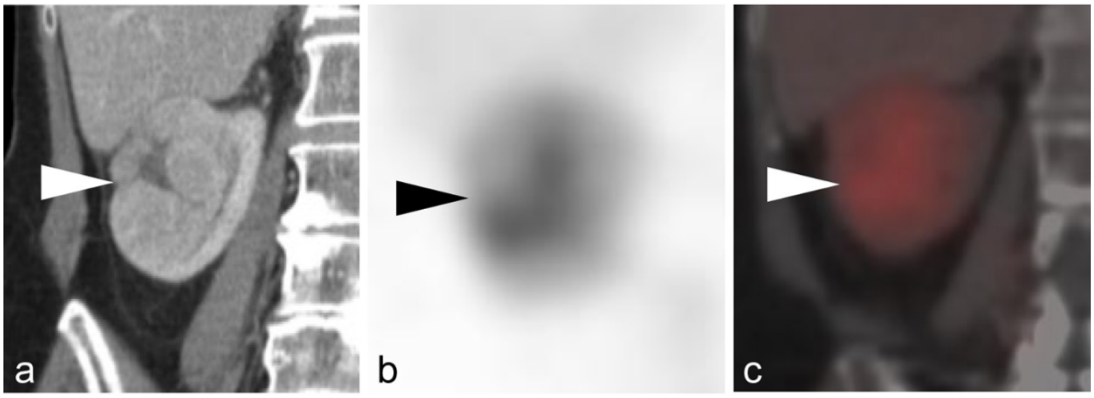

Figure 7: *(a) Coronal venous/nephrographic phase contrast-enhanced CT, (b) coronal ^{99m}Tc-sestamibi SPECT, and (c) coronal ^{99m}Tc-sestamibi SPECT/CT fusion images of a large renal mass (white and black arrowheads) with a stellate central scar. This pathology proven oncocytoma demonstrates the typical pattern seen in the context of the presence of a central scar, with predominantly peripheral radiotracer uptake and relative photopenia in the scar.*

(Figure and Figure legend courtesy of Br J Radiol: Scott P Campbell, Antonios Tzortzakakis, Mehrbod S Javadi, Mattias Karlsson, Lilja B Solnes, Rimma Axelsson, Mahamad E Allaf, Michael A Gorin, Steven P Rowe. 99mTc-sestamibi SPECT/CT for the characterisation of renal masses: a pictorial guide. Br J Radiol. 2018;91(1084):20170526)

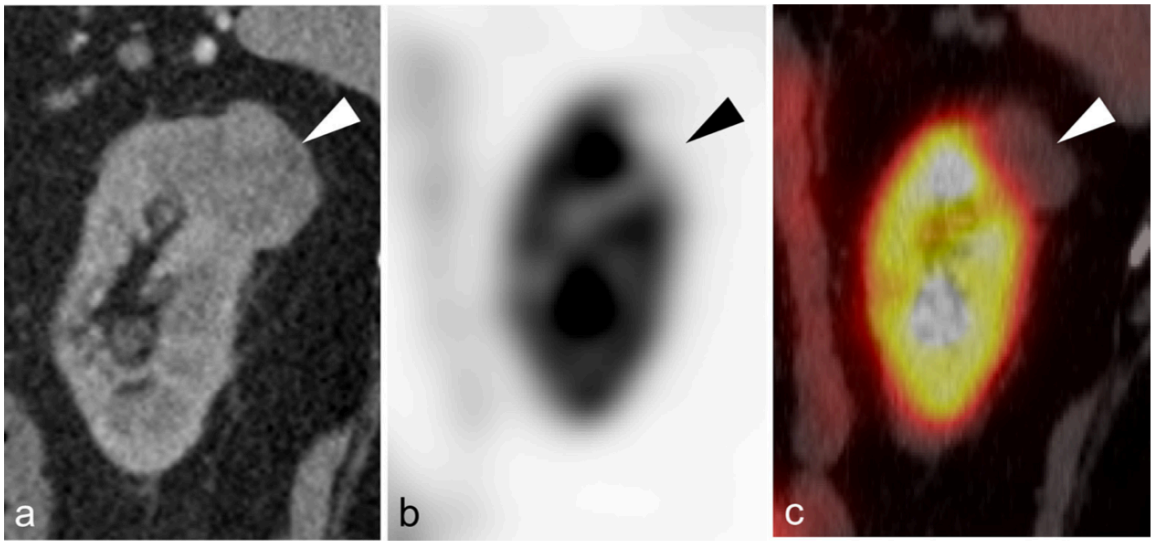

Figure 8: *(a) Sagittal arterial/corticomedullary phase contrast-enhanced CT, (b) sagittal ^{99m}Tc-sestamibi SPECT, and (c) sagittal ^{99m}Tc-sestamibi SPECT/CT fusion images of a predominantly exophytic photopenic (i.e., "cold") tumour (white and black arrowheads) with uptake markedly less than the adjacent normal renal parenchyma. This lesion was resected and was found to be a clear cell RCC.*

(Figure and Figure legend courtesy of Br J Radiol: Scott P Campbell, Antonios Tzortzakakis, Mehrbod S Javadi, Mattias Karlsson, Lilja B Solnes, Rimma Axelsson, Mahamad E Allaf, Michael A Gorin, Steven P Rowe. 99mTc-sestamibi SPECT/CT for the characterisation of renal masses: a pictorial guide. Br J Radiol. 2018;91(1084):20170526. doi:10.1259/bjr.20170526)

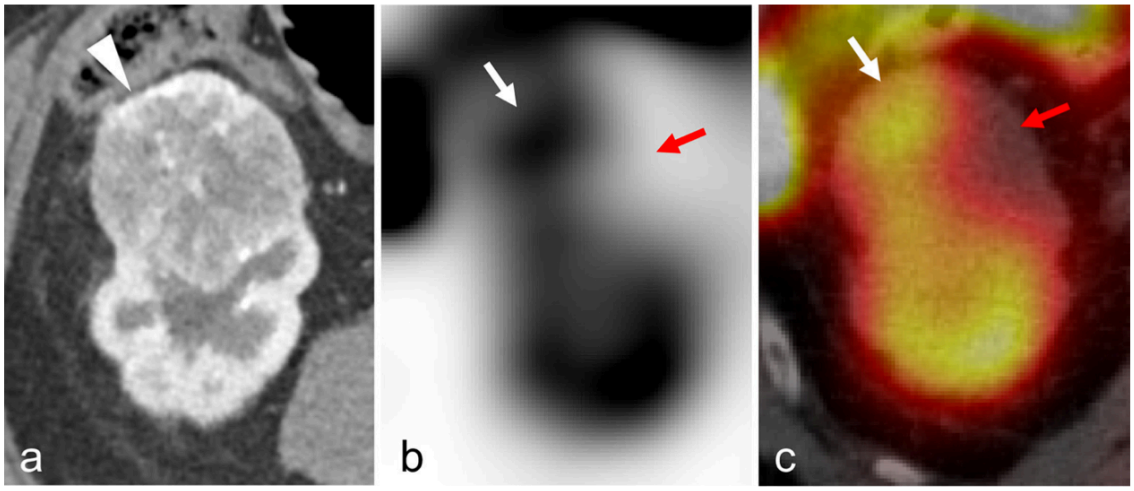

Figure 9: *(a) Axial arterial/corticomedullary phase contrast-enhanced CT, (b) axial ^{99m}Tc-sestamibi SPECT, and (c) axial ^{99m}Tc-sestamibi SPECT/CT fusion images demonstrating a tumour [white arrowhead in (a)] with heterogeneous uptake. Portions of the tumour have radiotracer uptake similar to renal parenchyma [white arrows in (b, c)] and other portions are distinctly low in uptake [red arrows in (b, c)]. This is another uptake pattern that suggests a benign or indolent lesion, and this tumour was found to be a HOCT upon resection.*

(Figure and Figure legend courtesy of Br J Radiol: Scott P Campbell, Antonios Tzortzakakis, Mehrbod S Javadi, Mattias Karlsson, Lilja B Solnes, Rimma Axelsson, Mahamad E Allaf, Michael A Gorin, Steven P Rowe. 99mTc-sestamibi SPECT/CT for the characterisation of renal masses: a pictorial guide. Br J Radiol. 2018;91(1084):20170526. doi:10.1259/bjr.20170526)

1.6 Histological characterisation of renal neoplasia

The number of core needle renal biopsy increases to reduce the overtreatment of benign renal tumours or when metastatic disease is present, in order to choose the suitable medical treatment [52]. The histological analysis by defining the subtype of RCC indicates the metastatic potential of the renal tumour, together with the tumour size and the sex of the patient [8]. Apart from the RCC subtype, histology indicates the nuclear grade [53] (e.g. Fuhrman grading system), the invasion of nearby tissue and vessels, the presence of sarcomatoid features as well as the presence of lymphadenopathy [20]. An accurate preoperative diagnosis of renal neoplasia appears to have difficulties, not only on imaging but also on histology grounds. In a metanalysis from Patel et al., 25% of RO diagnoses based on core biopsy reclassified as chRCC or HOCT after excision [14]. In that way, core biopsy becomes unreliable for a definite RO diagnosis since it represents a limited sample from the examined tumour tissue [52]. The differential diagnostic dilemma between RO and chRCC exist not only for material from core biopsies but also for nephrectomy specimens, emphasising in that way the limitations of histopathology and immunohistochemistry [54]. Other histology-based tools proposed for accurate differentiation of renal neoplasia apart from immunohistochemistry are in situ metabolomics [55], genomic approach [56] as well as computed assisted morphometry [57]. The last three mentioned tools are still on a research

level, and they are not used in everyday clinical praxis like histopathology and immunohistochemistry.

1.7 Treatment of renal neoplasia

Partial or radical nephrectomy is nowadays the only curative therapies for non-metastatic RCC with the former exhibiting better postoperative results in localised (T1a-b) tumours [20]. Active surveillance [58] and thermal ablation (percutaneous radiofrequency ablation or cryoablation) are alternative to surgery therapeutical approaches when the patient is unfit for surgery or when having small renal tumours [20]. Recent research from Bianchi et al. shows higher recurrence-free survival for patients with non-clear RCC and tumours smaller than 2cm when treated with partial nephrectomy or cryoablation than those treated with radiofrequency ablation [59]. Metastatic RCC requires systemic therapy (immunotherapy or targeted therapy mainly for ccRCC) whereas the effect of a cytoreductive nephrectomy is still under validation and ongoing research [60].

2 RESEARCH AIMS

General aim

The aim of this doctoral thesis is to explore if preoperative imaging with ^{99m}Tc-sestamibi SPECT/CT can have a beneficial role in the differential diagnosis of RO from RCC. To achieve that, our institution initiated during 2015 the MIDOR project (Molekylär Imaging för Differentiering av Onkocytom från Renal cancer, Drn 2015-01080) under the guidance of professor Rimma Axelsson. The Local Radiation Safety Committee and the Regional Ethics Review Board in Stockholm (Drn 2015/923-31/4) approved MIDOR study. In addition, our scientific group acquired written informed consent by all MIDOR project participants. VINNOVA financially supported MIDOR project and Hermes Medical Solutions Stockholm, Sweden introduced a new SUV SPECT® software enabling that way quantitative measurements on the examined MIDOR material. In that way, MIDOR project brought together different agencies (Karolinska Institutet, Karolinska University Hospital Huddinge, VINNOVA and Hermes Medical Solution) under a common goal to evaluate a new hybrid molecular technique in the field of renal oncologic imaging.

Study n.1

The first scientific paper aimed to examine whether the visual evaluation of ^{99m}Tc-sestamibi uptake from the examined renal tumours undergoing SPECT/CT examination can differentiate RO from RCC.

Study n.2

The second scientific paper evaluated the intra- and interobserver agreement of quantitative SUV SPECT measurements of the ^{99m}Tc-sestamibi uptake from the examined MIDOR material.

Study n.3

The principal aim of the third scientific paper was to evaluate if ^{99m}Tc-Sestamibi SPECT/CT combined with in-situ metabolomics analysis can characterise renal tumours exhibiting ^{99m}Tc-Sestamibi uptake.

Study n.4

The principal aim of the fourth paper was to investigate whether the addition of quantitative evaluation, namely SUV SPECT uptake from the examined MIDOR material could improve the diagnostic performance of ^{99m}Tc-Sestamibi SPECT/CT in the differentiation of RO from RCC.

3 MATERIALS AND METHODS

3.1 Recruitment of MIDOR participants

The Urology Department of Karolinska University Hospital, Huddinge was responsible for the recruitment of patients willing to participate in the MIDOR project. The total number of patients included was 52. This thesis has four scientific studies based on MIDOR participants that included gradually between 2015-2019. Inclusions criteria were common for the four studies, namely T1 renal tumours, smaller than 7cm in size, with no metastatic manifestations. All patients discussed in the multidisciplinary urological conference of the Radiology Department of Karolinska University Hospital, Huddinge and decision for nephrectomy (partial/total) or percutaneous kidney biopsy was taken. Before surgery or biopsy, the patients underwent a ^{99m}Tc-Sestamibi SPECT/CT examination in the Nuclear Medicine Department of Karolinska University Hospital, Huddinge.

3.2 Image acquisition

The same imaging protocol applied for all MIDOR participant concerning the ^{99m}Tc-Sestamibi SPECT/CT examination. Sixty to ninety minutes after the injection of 925 ± 25 MBq ^{99m}Tc-Sestamibi *(production and distribution: National Centre for Nuclear Research, Poland respectively S. Ahlén Medical Nordic AB, Stockholm, Sweden)* SPECT/CT imaging was performed. Image acquisition took place on a Siemens Symbia T16 *(Siemens Healthcare, Erlangen, Germany)* system equipped with low-energy high-resolution collimators. SPECT imaging was accomplished with a 128×128-pixel matrix size (zoom factor 1) and the acquisition of 64 projections in a step-and-shoot mode, during a 40 seconds time frame for each projection. CT imaging for attenuation correction and anatomical correlation followed the SPECT acquisition, using 130 kV tube voltage and a 5mm slice width. To provide proper tube current modulation with a quality reference mAs setting of 10, the automatic exposure control CARE Dose4D was activated. [61]. The iterative OSEM algorithm (6 iterations, 16 subsets) was applied for scatter correction. After the attenuation and collimator resolution, post-filtration was performed using a Gaussian 3D-filter (8 mm full-width at half-maximum). Information about syringe activity, residual activity in the syringe, patient weight, time points of injection and scan start were acquired to perform the quantitative evaluation. The data above were specified in the reconstruction software. The reconstruction of SPECT and CT data acquired, performed with *HERMES Hybrid Recon™ Oncology v.1.1B (HERMES Medical Solutions AB, Stockholm, Sweden).* ^{99m}Tc-Sestamibi SPECT/CT examinations were visually evaluated twice by two independent readers and measurements of ^{99m}Tc-Sestamibi uptake in the renal tumour and the non-tumoral kidney parenchyma performed within a one-week interval in *HERMES Hybrid Viewer PDR v2.5.*

3.3 Study n.1

Twenty-four patients included in the first pilot study of this thesis. Four patients had multiple bilateral tumours resulting in a total of 31 kidney tumours to be evaluated. In this first scientific study, a visual assessment of ^{99m}Tc-Sestamibi uptake from the examined kidney tumours was performed blindly within a one-week period, once by a professor in nuclear medicine and once by a senior consultant radiologist. Our scientific group decided that any focal ^{99m}Tc-Sestamibi uptake from the renal tumour was considered as positive (Sestamibi

positive), whereas tumours with ^{99m}Tc-Sestamibi uptake lower than non-tumoral kidney parenchyma was considered as negative (Sestamibi negative). The results of the above-mentioned visual assessment correlated subsequently with the clinical, histopathological results from the surgical specimens or the biopsy material.

3.4 Study n.2

Forty-eight kidney tumours from patients participating in the MIDOR project were included in the second scientific study. Standard uptake value (SUV) measurements were performed by freehand drawing regions of interest (ROI) at the site of the renal tumour and the ipsilateral non-tumoral kidney parenchyma on the axial fused SPECT/CT images as shown on **Fig**.10. Subsequently, volumes of interest (VOIs) based on the manually drawn ROIs were generated from the software, extracting at the same time SUV_{max}, SUV_{mean} and SUV_{peak} for the renal tumours and the non-tumoral kidney parenchyma (**Fig**.11). The level of agreement among the different SUV measurements was evaluated by calculating the intraclass correlation coefficient (ICC) [62].

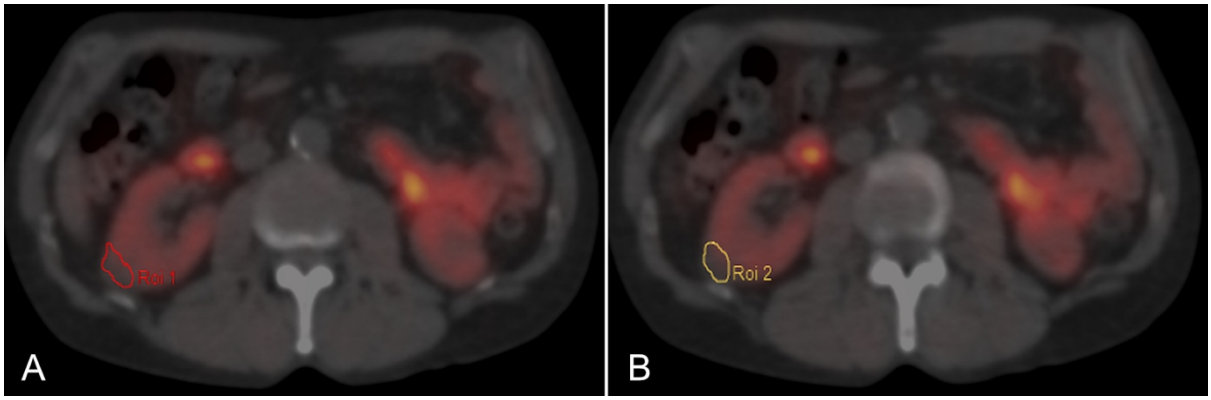

Figure 10: Manual drawing (A, B) in two different regions of interest (ROI), at the site of the tumour in the right kidney.

Figure 11: Volumes of interest (VOIs) based on the manually drawn ROIs (A) were generated from the software, extracting at the same time SUV_{max}, SUV_{mean} and SUV_{peak} for the tumour on the right kidney (**Fig**.10) and the non-tumoral kidney parenchyma (B).

3.5 Study n.3

A complimentary approval by the Regional Ethics Review Board in Stockholm (2018/1626) and the Stockholm Biobank (Bbk 2082) along with a newly signed informed consent form were obtained before the beginning of the third scientific study.

Tumour material from MIDOR participants was retrieved, namely haematoxylin & eosin (HE), as well as immunohistochemistry (IHC), slides from the archives of Clinical Pathology-Cytology Department Karolinska University Hospital in Huddinge. Two independent histopathologists reviewed the whole MIDOR material, and their diagnosis was utilised as the gold standard to which visual assessment ^{99m}Tc-Sestamibi SPECT/CT results and in-situ metabolomics data were compared. Tissue microarray analysis (TMA) of 33 tumour samples from 28 patients included in the third scientific study to investigate their in-situ metabolome status. *Research Unit Analytical Pathology (Helmholtz Zentrum München) performed matrix-assisted laser desorption/ionisation (MALDI) mass spectrometry imaging (MSI) analysis*, as described previously by Ly et al. [63]. To validate emerging data, we used part of a previously published cohort, comprising 117 tumours: 59 ROs and 58 chRCCs. Metabolomic differences found between Sestamibi positive and Sestamibi negative chRCCs gave rise to an additional review from an expert urological histopathologist [64]. MALDI MSI data analysis, as well as image generation, was facilitated by FlexImaging v. 4.2. K-means analysis was performed by SCiLS Lab software, followed by R-package CARRoT analysis to assess the highest predictive power in the differential of RO from chRCC. Heatmap-based clustering, s-PLSDA and volcano plots were created with MetaboAnalyst 3.0.

3.6 Study n.4

In the fourth scientific study of MIDOR project, 58 renal tumours from 52 patients were included [62]. In this final assessment, two readers evaluated the MIDOR material, both

visually and quantitatively. To improve interobserver variation concerning the visual evaluation, we defined the uptake of ^{99m}Tc-Sestamibi from the examined renal tumour, as follows: a tumour was classified as Sestamibi-positive if the ^{99m}Tc-Sestamibi uptake was higher compared to ipsilateral non-tumoral renal parenchyma. If the uptake from the renal tumour was equal to, or lower than ipsilateral renal parenchyma, then the tumour was classified as Sestamibi-negative.

Quantitative evaluations were performed by measuring SUV_{mean} and SUV_{max} in the renal tumour and the ipsilateral non-tumoral renal parenchyma. Freehand ROIs were drawn manually in the CT images of the SPECT/CT examination and not on the fused image like in previous study 2, including the whole renal tumour. Volumes of interest (VOIs) were automatically generated, and SUV-parameters were noted. In this study, fixed 1cm^3 VOIs spheres were preferred and drawn manually in regions of high ^{99m}Tc-Sestamibi uptake to obtain SUV_{mean} and SUV_{max} values of the ipsilateral non-tumoral renal parenchyma. SUV_{peak} measurements were not included since many tumours were too small in volume (approximately 1cm^3) to be evaluated with this parameter as by definition SUV_{peak} represents the maximum ^{99m}Tc-Sestamibi activity concentration in a 1cm^3 volume within a larger VOI.

MIDOR's histopathological material (surgical resection specimens and/or biopsies) was re-evaluated. Two consultant histopathologists independently reviewed HE as well as IHC slides of all tumours in a blinded manner. Their histopathological diagnoses were correlated with the results from the visual assessment of ^{99m}Tc-Sestamibi SPECT/CT examinations. A third histopathologist, who is an expert in renal neoplasia, was asked to blindly evaluate all chRCCs included in this study since in situ metabolomic differences in Sestamibi-positive versus Sestamibi-negative chRCCs have been found [64].

To evaluate the mitochondrial content of renal oncocytic tumours that appear to be positive in ^{99m}Tc- Sestamibi examination, succinate dehydrogenase complex subunit B (SDHB) protein expression was used since IHC can detect SDHB protein expression. Samples from 19 tumours (9 RO, 3 HOCTs and 7 chRCCs) previously arranged in a TMA format were utilised [64].

ICC was evaluated to assess the intra-reader reliability of the different SUV measurements in the renal tumour and the non-tumoral renal parenchyma. Consequently, we calculated the average value between the two separate measurements ($SUV_{max,}$ respectively SUV_{mean} SPECT/CT) from each reader per patient. This average value was used in our analysis as well as the ratio of the relative ^{99m}Tc- Sestamibi uptake (rate of SUV_{max} respectively SUV_{mean} uptake from the renal tumour / SUV_{max} respectively SUV_{mean} uptake from ipsilateral non-tumoral renal parenchyma). Receiver operating characteristic (ROC) curve analysis was used to exemplify and understand the trade-off in sensitivity and specificity of Sestamibi-positive vs Sestamibi-negative renal tumours. To demonstrate the illustration of the results in an easy way, each tumour category was designated with a letter, namely A-J (**Fig.**12).

The SDHB score was analysed both as a categorical and numerical variable. Categorical SDHB (ranging from 0 to 4) was analysed with Fisher's Exact Test, and numerical SDHB was analysed with Wilcoxon Sum Rank Test.

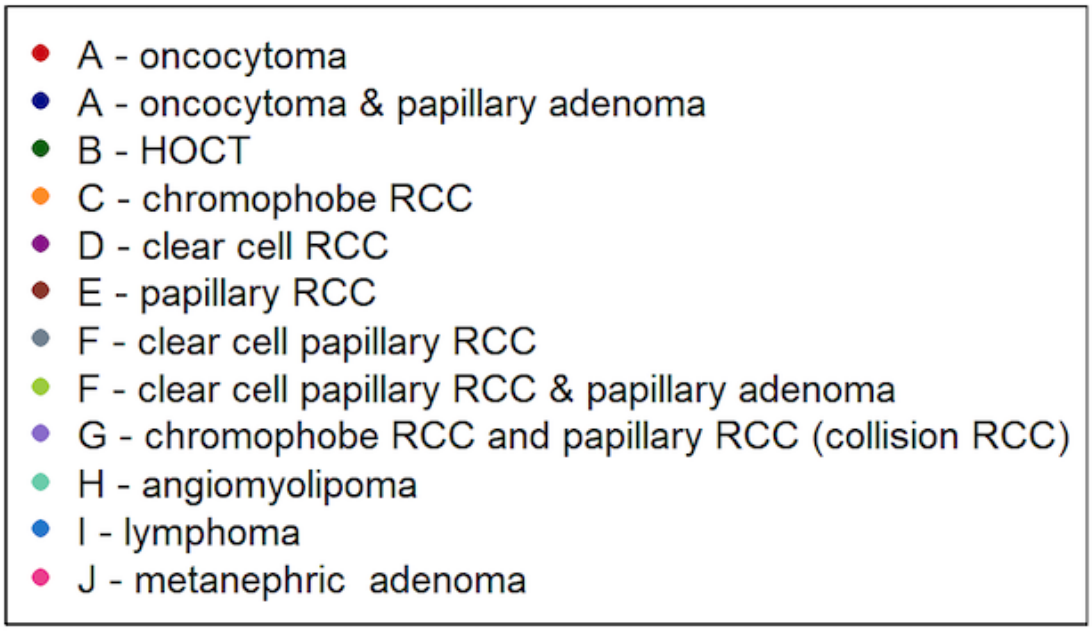

Figure 12: Different renal tumour categories assigned with a letter, namely A-J.

4 RESULTS

4.1 Study n.1

Sixteen out of 31 lesions underwent partial or total nephrectomy. The remaining 15 were biopsied—the results of the visual evaluation correlated with the clinical, histopathological diagnosis. According to our initial hypothesis, renal tumours that were categorised as Sestamibi positive were most probably RO whereas Sestamibi negative tumours were most probably RCC. The results of the visual evaluation are summarised in **Table** 1. Like in other similar studies HOCT were also Sestamibi positive. One pRCC had slightly increased ^{99m}Tc- Sestamibi uptake.

Type of lesions	**Number of lesions**	**Sestamibi positive**	**Sestamibi negative**
RO	12 (39%)	11 (91,6%)	1 (8,4%)
HOCT	3(10%)	3 (100%)	0
Metanephric adenoma	1(3%)	0	1 (100%)
Lymphoma	1(3%)	0	1 (100%)
AML	1(3%)	1 (100%)	0
ccRCC	7(23%)	0	7 (100%)
pRCC	3(10%)	1 (33,3%)	2 (66,7%)
ChRCC	2(6%)	0	2 (100%)
Collision (chromophobe RCC – papillary RCC)	1(3%)	0	1 (100%)

Table 1: Visual evaluation of 31 renal tumours in terms of Sestamibi uptake resulting in a 91.6% sensitivity and 94,7% specificity concerning the differentiation of RO.

4.2 Study n.2

Tables 2-4 summarises the ICC values as well as their upper and lower margins extracted from SUV SPECT measurements, performed by the two readers on the solid renal tumours and the ipsilateral non-tumoral renal parenchyma.

SUV_{mean}:

As presented in **Table 1a**, ICC concerning the SUV_{mean} measurements of the solid renal tumour (T) in the same reader varies between 95%-98%. The ICC of SUV_{mean} measurements on the ipsilateral healthy renal parenchyma (N) varies between 93%-98%.

Test-retest same reader	ICC	Lower	Upper
Reader 1 - T	0.984	0.972	0.991
Reader 2 - T	0.954	0.920	0.974
Reader 1 - N	0.975	0.956	0.986
Reader 2 - N	0.932	0.883	0.961

Table 2a: ICC for repeated measurements of SUV_{mean} by the same reader.

T: renal tumour, N: non-tumoral renal parenchyma

Table 2b exhibits that ICC between readers concerning SUV_{mean} measurements of the renal tumours varies between 86%-89%. The ICC of SUV_{mean} measurements on the ipsilateral healthy renal parenchyma between readers was found to be 73%.

Between readers	ICC	Lower	Upper
First measurement - T	0.890	0.814	0.936
First measurement - N	0.732	0.530	0.848
Second measurement - T	0.858	0.762	0.917
Second measurement - N	0.734	0.560	0.843

Table 2b: ICC for repeated measurements of SUV_{mean} between readers.

SUV_{peak}

Tables 3a and 3b show ICC values for SUV_{peak} measurements by the same reader and between readers, respectively.

Test-retest same reader	ICC	Lower	Upper
Reader 1 - T	0.989	0.980	0.994
Reader 2 - T	0.969	0.946	0.982
Reader 1 - N	0.982	0.968	0.989
Reader 2 - N	0.932	0.884	0.961

Table 3a: ICC for repeated measurements of SUV_{peak} by the same reader.

Between readers	ICC	Lower	Upper
First measurement - T	0.887	0.809	0.934
First measurement - N	0.705	0.526	0.823
Second measurement - T	0.915	0.856	0.951
Second measurement - N	0.656	0.447	0.794

Table 3b: ICC for repeated measurements of SUV_{peak} between readers.

SUV_{max}

ICC concerning the SUV_{max} measurements of solid renal tumours in the same reader varies between 97%-99%. The ICC of SUV_{max} measurements on the ipsilateral healthy renal parenchyma varies between 92%-98% (**Table 4a**).

Test-retest same reader	ICC	Lower	Upper
Reader 1 - T	0.989	0.981	0.994
Reader 2 - T	0.965	0.939	0.980
Reader 1 - N	0.983	0.970	0.990
Reader 2 - N	0.921	0.865	0.954

Table 4a: ICC for repeated measurements of SUV_{max} by the same reader.

ICC between readers concerning SUV_{max} measurements of the renal tumours varies between 87%-89%. The ICC of SUV_{max} measurements on the ipsilateral healthy renal parenchyma between readers was 72%-73% (**Table 4b**).

Between readers	ICC	Lower	Upper
First measurement - T	0.866	0.775	0.922
First measurement - N	0.715	0.518	0.835
Second measurement - T	0.890	0.812	0.936
Second measurement - N	0.729	0.524	0.847

Table 4b: ICC for repeated measurements of SUV_{max} between readers.

4.3 Study n.3

The results of the visual assessment of renal tumours examined with ^{99m}Tc- Sestamibi SPECT/CT in the third scientific study are presented in **Table 5**. Of note is that the single pRCC exhibiting slight ^{99m}Tc- Sestamibi uptake in the first scientific study was reclassified as chRCC upon re-evaluation on histopathological grounds.

Tumour type	No. of renal tumours	^{99m}Tc-Sestamibi positive, n (%)	^{99m}Tc-Sestamibi negative, n (%)
RO	9	7 (78%)	2 (22%)
HOCT	3	3 (100%)	0
chRCC	7	3 (43%)	4 (57%)
ccRCC	6	0	6 (100%)
pRCC (type 1)	8	0	8 (100%)

Table 5. Visual assessment of 33 renal tumours examined with ^{99m}Tc- Sestamibi SPECT/CT included in the third scientific study.

A discriminatory metabolomic signature for positive on ^{99m}Tc-Sestamibi SPECT/CT Birt-Hogg-Dubè (BHD)-associated HOCT vs other renal oncocytic tumours was identified. Evident metabolomic differences found between ^{99m}Tc-Sestamibi positive and negative chRCCs that prompted an additional expert review; two of three ^{99m}Tc-Sestamibi positive chRCCs were reclassified as LOT, which is an emerging RCC entity (**Fig**.13). Metabolomic differences were found between distal-derived tumours (i.e., chRCC) from those of proximal tubule origin (i.e., ccRCC and pRCC), including differences between RO and chRCC.

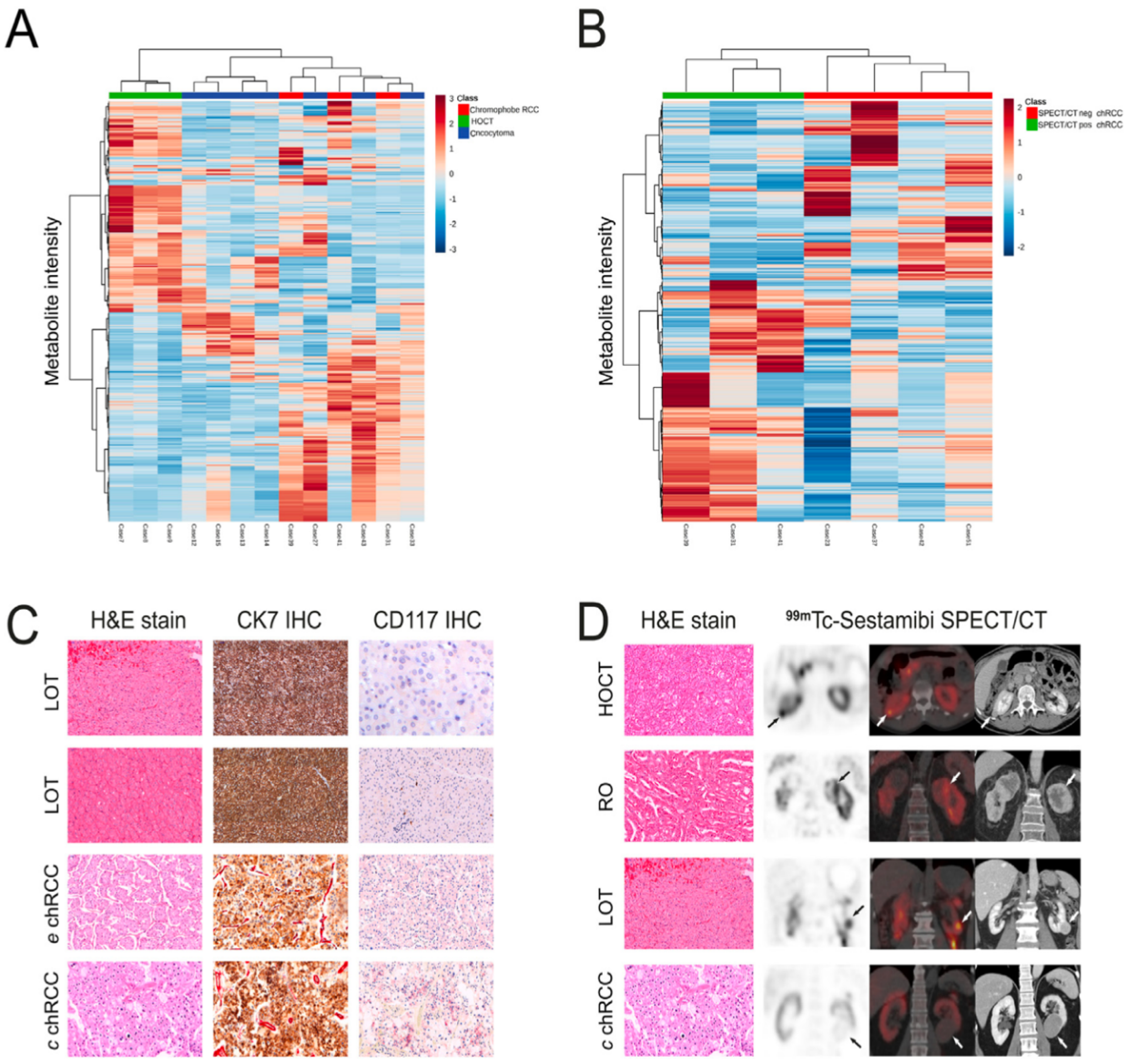

Figure 13: *Metabolomic Data Analysis Segregates ^{99m}Tc-Sestamibi SPECT/CT positive BHD-associated HOCTs and distinguishes SPECT/CT positive LOTs from classic chRCCs. (A) Unsupervised clustering analysis based on discriminative metabolites (n=460) depicting a clear separation between ^{99m}Tc-Sestamibi SPECT/CT positive BHD-associated HOCTs vs other ^{99m}Tc-Sestamibi SPECT/CT negative renal oncocytic neoplasms; (B) Heatmap of top 420 m/z values highlights different m/z expression patterns in SPECT/CT photophilic chRCCs versus photopenic counterparts; (C) These in situ metabolomic differences prompted a pathologic evaluation of all chRCCs: Histopathological features of three ^{99m}Tc-Sestamibi SPECT/CT positive chRCCs (cases No 41, 31 and 39; top to bottom) which were amended to LOTs (cases No 41 & 31) and eosinophilic chRCC (case No 39) upon expert review. A ^{99m}Tc-Sestamibi SPECT/CT negative classic chRCC (case No 51) is also included in the panel (bottom); (D) Histological features and hybrid molecular imaging (scintigraphic, SPECT/CT and CT study) of three ^{99m}Tc-Sestamibi SPECT/CT positive cases: HOCT (case No 8: axial view of 13 mm tumour on the dorsal aspect of right kidney exhibiting ^{99m}Tc-Sestamibi uptake), RO (case No 14: coronal view of 60 mm tumour with a necrotic component on the upper pole of left kidney exhibiting ^{99m}Tc-Sestamibi uptake), and LOT (case No 41: coronal*

view of 28 mm tumour on the lower pole of left kidney exhibiting ^{99m}Tc-Sestamibi uptake), as well as ^{99m}Tc-Sestamibi SPECT/CT negative classic chRCC (case No 51: coronal view of 64 mm tumour on the medial aspect of the lower pole of left kidney without ^{99m}Tc-Sestamibi uptake; top to bottom).

(Figure and Figure legend courtesy of Papathomas T, Tzortzakakis A, Sun N, Erlmeier F, Bozoky B, Kokaraki G, et al. In Situ Metabolomics Expands the Spectrum of Renal Tumours Positive on 99m Tc-sestamibi Single Photon Emission Computed Tomography / Computed Tomography Examination. Eur Urol Open Sci. European Association of Urology.; 2020;22:88–96)

4.4 Study n.4

Five renal tumours reclassified upon re-evaluation by consensus: 4 RO were reclassified as chRCC and HOCT (2 cases each), while one papillary RCC reclassified as chRCC. Another renal mass previously characterised as HOCT corresponded to healthy renal parenchyma and thus excluded from further analysis reducing the total number of tumours to 57.

Accordingly, the final diagnoses were established as follows: 13 ccRCCs, 11 chRCCs, 11 RO (one with adjacent) papillary adenoma, 9 pRCCs, 5 HOCTs, 4 ccpRCCs (one with adjacent papillary adenoma), 1 “collision tumour” comprising chromophobe RCC with adjacent pRCC, 1 B cell non-Hodgkin’s (follicular) lymphoma, 1 metanephric adenoma and 1 AML.

Agreement between the readers concerning the visual evaluation of ^{99m}Tc-Sestamibi uptake was observed in 51 out of 57 (89.5%) solid renal tumours. In 6 (10.5%) cases, the two readers were in disagreement. A third reader with a nuclear medicine background was introduced, and all three readers independently performed a blind re-evaluation of those six cases: a complete agreement was achieved between the two readers with a nuclear medicine background, and the final consensus was reached (**Table** 6).

Histological types of renal tumours	Number of renal tumours	^{99m}Tc- Sestamibi positive, n (%)	^{99m}Tc- Sestamibi negative, n (%)
RO	11	9 (82%)	2 (18%)
HOCT	5	5 (100%)	0
chRCC	11	6 (55%)	5 (45%)
ccRCC	13	0	13 (100%)
pRCC	9	0	9 (100%)
ccpRCC	4	0	4 (100%)
Collision RCC	1	0	1 (100%)
B-cell Lymphoma	1	0	1 (100%)
Metanephric adenoma	1	0	1 (100%)
AML	1	0	1 (100%)

Table 6: Visual evaluation of ^{99m}Tc-Sestamibi uptake on 57 solid renal tumours resulting in 82% sensitivity and 76% specificity concerning the differentiation of RO.

Similar to our previously scientific study 2, the ICC for SUV_{max} and SUV_{mean} measurements between the two readers showed a high agreement of 88% and 94%, respectively. Likewise, the ICC between the readers, when measuring SUV parameters in the ipsilateral non-tumoral renal parenchyma showed moderate agreement.

Statistical analysis of the quantitative evaluation revealed significant results (*p-value* less than 0.001) in $SUV_{max,}$ and SUV_{mean} SPECT/CT measurements performed on renal tumours and the non-tumoral renal parenchyma. ROC curve analyses based on the ratio of the relative ^{99m}Tc-Sestamibi uptake were performed by sub-clustering RO as a SPECT/CT positive subgroup (subgroup A). At the same time, all remaining tumour types were considered a SPECT/CT negative subgroup. Cut-off values for the characterisation of RO as Sestamibi-positive vs all the rest tumours subgroups were obtained. The ratio of relative ^{99m}Tc-Sestamibi uptake based on SUV_{max} measurements of the tumour (T) vs non-tumoral renal parenchyma (N) demonstrated the best performance under the curve (0.787) (**Fig.** 14) compared to other ROC analyses based only on SUV_{mean} measurements.

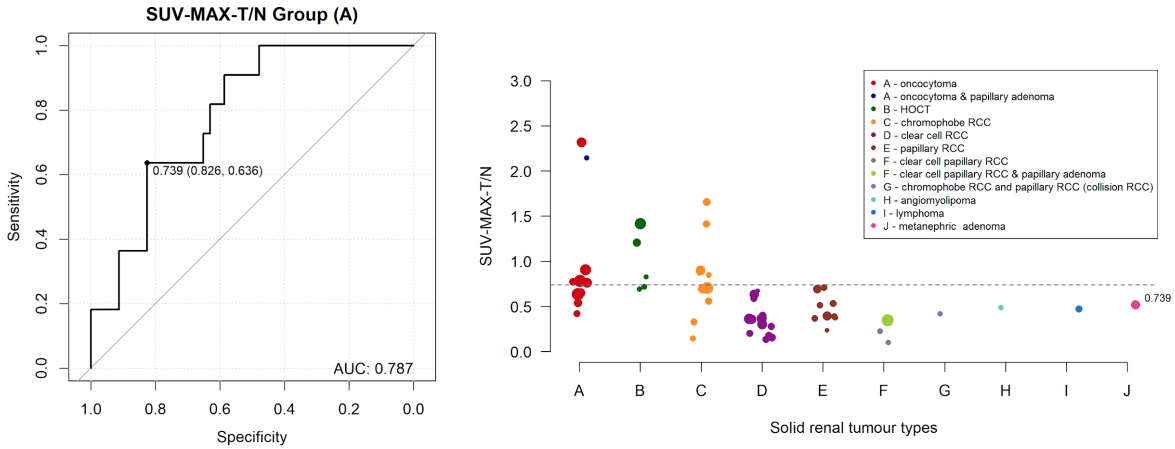

Figure 14: Ratio of relative ^{99m}Tc-Sestamibi uptake based on SUV_{max} measurements on the renal tumour (T) and the non-tumoral renal parenchyma (N). Quantitative evaluation of SUV_{max} measurements of ^{99m}Tc-Sestamibi uptake on 57 solid renal tumours resulted in 64% sensitivity and 83% specificity in detecting RO.

One expert urological histopathologist re-evaluated all chRCCs: five renal Sestamibi-negative tumours were classified as 4 chRCCs classic type and 1 as an eosinophilic variant of chRCC. Six Sestamibi-positive tumours were reclassified as 3 LOTs, 2 as eosinophilic variants of chRCC and 1 chRCC classic type. However, all these tumours were included in the chRCC subgroup given that LOT represents an emerging renal tumour entity that has been recently proposed, which awaits formal acceptance and potential inclusion in the WHO classification [65].

The median SDHB score in the Sestamibi positive group was 4 vs 3 in the negative group, with the most common value being 4 in the former and 3 in the latter. A trend of higher SDHB values in the positive group was found compared to the negative group (p=0.183 vs p=0.071). A linear-by-linear association test, to keep SDHB as a categorical variable taking the order of values into account, suggested a significant trend (p=0.038). There was no statistically significant difference in the SDHB immune expression patterns between the tumour types (p=0.738).

5 DISCUSSION

Study n.1

Our data confirmed the hypothesis that RO show ^{99m}Tc-Sestamibi uptake in SPECT/CT examination resulting in a high sensitivity of nearly 92%, which was in accordance with other published studies at that time [47,48]. The three Sestamibi positive HOCTs was another common finding with the studies mentioned above from John Hopkins scientific group [48]. HOCT constitutes a subtype of chRCC without any evidence of metastatic potential although no publications with follow-ups longer than ten years exist [66]. HOCT is an emerging renal entity which is distinct from RO and chRCC [11]. The presence of false-positive results indicated the eventual need for quantitative tools in addition to visual assessment for more accurate characterisation of renal neoplasia. Hermes Medical Solutions Stockholm, Sweden introduced SUV SPECT® software that could enable quantitative evaluation of the examined MIDOR material leading our group to continue with the second scientific study to validate the measurements performed by the software mentioned above.

Study n.2

SUV SPECT® software from Hermes Medical Solutions enables SUV SPECT measurements on the examined renal tumours resulting in ICC between readers to be around 85%-90%. That means that 85%-90% of the observed variability is mostly due to actual variability among the examined tumours, and only about 10%-15% is due to variability between readers. A 10%-15% variability in the measurements between readers is a percentage of measurement error which is acceptable in everyday clinical praxis. The intrinsic limitations of SPECT/CT examination, the difficulty in drawing the ROIs manually on the fused SPECT/CT images especially in small-sized renal tumours, the challenges in obtaining SUV_{peak} values mainly in small-sized tumours and the heterogenicity of larger renal tumours were the main limitations revealed in this second scientific study. The strong agreement among the different SUV measurements performed on MIDOR material encouraged our group to utilize quantitative tools besides visual assessment of ^{99m}Tc-Sestamibi uptake from the examined kidney tumours and non-tumoral kidney parenchyma.

Study n.3

In this third scientific study, we suggested an *in-situ* metabolomic analysis of renal tumours previously examined with ^{99m}Tc-Sestamibi SPECT/CT examination. This resulted in the expansion of ^{99m}Tc-Sestamibi positive renal tumours encompassing RO, HOCT, LOT and chRCC, supporting in that way combined diagnostics that utilise molecular imaging and histometabolomic profiling. Two ^{99m}Tc-Sestamibi positive cases initially considered chRCC (eosinophilic type) clustered together and separately from the negative classic chRCCs; both were reclassified as LOTs upon expert review. Three BHD-associated HOCT cases also exhibited distinct metabolomic profile, further reinforcing the concept that HOCT may represent a unique renal entity and not a chRCC subtype/variant, according to the current WHO classification. The principal limitation of this study was the small number of cases investigated using both ^{99m}Tc-Sestamibi SPECT/CT and MALDI-MSI with a variable representation of tumour entities. Nevertheless, the diverse metabolic profiles and behaviour of chRCC which may appear both Sestamibi positive and Sestamibi negative on ^{99m}Tc-

Sestamibi SPECT/CT examination, generated a closer look to this indolent RCC subgroup and the description of an emerging RCC entity namely LOT (**Fig.** 15).

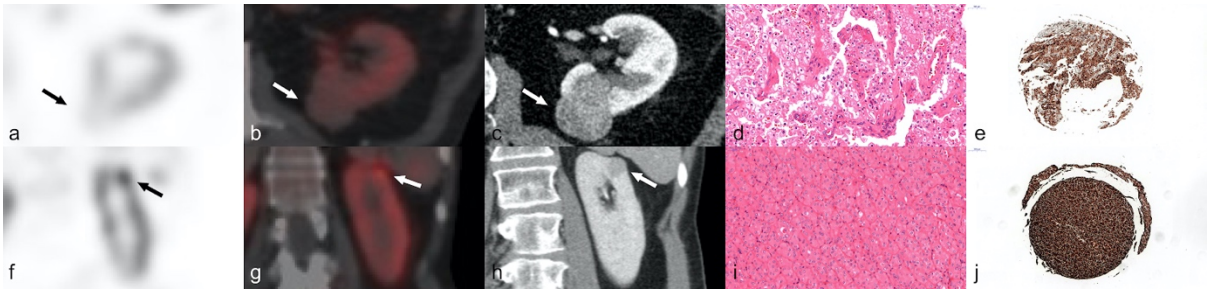

Figure 15*:* One Sestamibi-negative and one Sestamibi-positive chRCC.

First row, a-e: (case 42) SPECT axial image (a) indicates the absence of radioisotope in a classic chromophobe RCC located at the dorsal aspect of the left kidney (indicated by arrow). Fused axial SPECT/CT images (b), white arrow indicates the tumour. Preoperative axial CECT image (c) in the venous phase, white arrow indicates the tumour. Histological sections of the tumour characterised as a chRCC (d-e) upon expert review.

Second row, f-j: (case 31) SPECT coronal image (f) indicates focal radioisotope uptake in a chromophobe RCC located at the upper pole of the left kidney (indicated by arrow). Fused axial SPECT/CT images (g), white arrow indicates the tumour. Preoperative axial CECT image (h) in the venous phase (white arrow indicates the tumour). Histological sections of the tumour (i-j) re-characterised as a typical example of LOT upon expert review.

Study n.4

Quantitative evaluation with SUV SPECT measurements did not improve the performance of ^{99m}Tc-Sestamibi SPECT/CT examination in differentiating RO from RCC compared to visual evaluation. All HOCTs and approximately half of the chRCC cases were classified as Sestamibi-positive, raising the question of clinical importance of how often tumours with an indolent clinical course might be misclassified (**Fig**.16). This finding could be eventually incorporated into modern active surveillance programs to reduce the overtreatment of benign renal tumours. In this study, a semi-quantitative immunohistochemical analysis of the mitochondrial content did not yield any significant differences between Sestamibi-positive and Sestamibi-negative renal tumour subsets, possibly attributed either to the functional status of the mitochondria or to the intra-tumoral heterogeneity, given the limited tumour sampling.

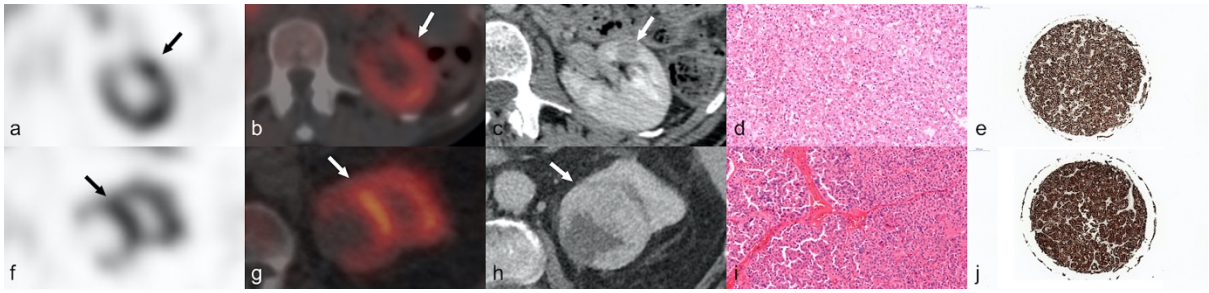

Figure 16: A RO and a HOCT, both positive on ^{99m}Tc-Sestamibi SPECT/CT.

First row, a-e: (case n.9) The scintigraphy study (a) displays an axial view of focal radioisotope uptake in the anterior aspect of the left kidney (indicated by arrow). Anatomic correlation of the previous uptake (c) in the CT study, axial view-venous phase. The axial SPECT/CT fusion image (b) with ^{99m}Tc-Sestamibi uptake in the same solid renal neoplasm (12mm in maximum diameter) of the left kidney. This was subsequently diagnosed as HOCT on histopathology (d-e).

Second row, f-j: (case n.13) The scintigraphy study (f) displays a coronal view of focal radioisotope uptake in the upper pole of the left kidney (indicated by arrow). Anatomic correlation of the previous uptake (h) in the CT study, axial view-venous phase. The axial SPECT/CT fusion image (g) with ^{99m}Tc-Sestamibi uptake in the same solid renal neoplasm (69mm in maximum diameter) of the left kidney. This was subsequently diagnosed as RO on histopathological grounds (i-j).

6 CONCLUSIONS

Study n.1

The visual interpretation of ^{99m}Tc-Sestamibi SPECT/CT shows clear benefits as a new diagnostic tool in the characterisation of renal neoplasia. Renal tumours without uptake of ^{99m}Tc-Sestamibi on SPECT/CT have most probably a malignant character, whereas renal tumours with ^{99m}Tc-Sestamibi uptake are likely benign.

Study n.2

SUV SPECT measurements on the renal tumours of MIDOR material performed in *HERMES Hybrid Viewer PDR v2.5* showed high ICC values around 90%. Those high ICC values indicate a strong agreement among the different SUV measurements for patients with renal tumours examined with ^{99m}Tc-Sestamibi SPECT/CT.

Study n.3

The third scientific study by supporting the feasibility of an integrated in-situ metabolomic profiling for the characterisation of renal tumours provides novel molecular insights into renal neoplasia. Our research suggests that renal tumours positive on ^{99m}Tc-Sestamibi SPECT/CT should be biopsied and analysed in an integrated fashion to guide further clinical decisions. New emerging renal entities like LOTs appear to have different metabolic signatures compared to already known RCC subtypes that correlate with their ^{9m}Tc-Sestamibi SPECT/CT misclassification.

Study n.4

Quantitative evaluation with SUV SPECT measurements did not improve the performance of visual evaluation on a ^{99m}Tc-Sestamibi SPECT/CT examination in characterising RO and differentiating this benign renal tumour from RCC. Visual evaluation of ^{99m}Tc-Sestamibi SPECT/CT identifies a larger Sestamibi-positive tumour group containing RO, HOCT and the majority of chRCCs. Sestamibi-negative renal tumours should be considered for surgery. On the other hand, Sestamibi-positive renal tumours could be suited for biopsy or follow up according to modern surveillance protocols. Emerging new renal tumour entities such as LOT appear to be positive on ^{99m}Tc-Sestamibi SPECT/CT examination.

7 POINTS OF PERSPECTIVE

Research projects like MIDOR is a clear example of how Academic structure, Clinical praxis and Private sectors can cooperate to achieve novel, beneficial results for the health care system and subsequently the society. Similar future efforts should be promoted and encouraged when clear rules and roles for the different counterparts exist.

John Hopkins's scientific group and Karolinska's MIDOR study were the first to demonstrate the beneficial role of ^{99m}Tc-Sestamibi SPECT/CT in the characterisation of renal neoplasia and how hybrid imaging could contribute in the reduction of overtreating benign renal tumours [43,44]. During the past year more scientific groups have published similar results [67–69] underlining the increasing interest in this field of renal oncologic imaging.

In accordance with the studies mentioned above, our scientific team concluded that ^{99m}Tc-Sestamibi SPECT/CT points out a larger group of renal tumours that show ^{99m}Tc-Sestamibi uptake. This group contains renal tumours of indolent clinical course like RO, HOCT and chRCC. At the same time, ^{99m}Tc-Sestamibi SPECT/CT followed by in situ metabolomic analysis added valuable evidence in an emerging renal tumour subcategory which is metabolically unique, namely LOT [64] since we observed different metabolic signatures between Sestamibi positive and Sestamibi negative chRCCs.

Nowadays, a large number of publications indicate that ROs are Sestamibi positive. Patients with Sestamibi positive renal tumours could avoid or postpone surgical treatment. Instead, a renal biopsy could be preferred as well as a longer follow up period to track the dynamics of the examined renal neoplasia.

Further metabolomic analyses in bigger tumour samples could contribute to distinct metabolic signatures, increasing in that way the confidence of a renal biopsy. For example, our study indicated a unique metabolic profile for HOCT from a single BHD patient. It would be interesting to know if that is the general case for HOCT. LOT is another emerging renal tumour entity that should be examined and further characterised in clinical settings to ascertain its assumed indolent character.

A recent cost-effectiveness analysis [70] indicates that modern cancer track algorithms in urologic oncology should include ^{99m}Tc-Sestamibi SPECT/CT examination since there are clear financial and diagnostic benefits from its use. The knowledge mentioned above that ^{99m}Tc-Sestamibi SPECT/CT brings in the characterisation of renal neoplasia followed by a confirmatory renal biopsy can reduce not only the overtreatment of benign renal tumours but also reduce the percentage of untreated malignant renal tumours.

8 ACKNOWLEDGEMENTS

I would like to thank **every single patient** that took part in the MIDOR project. The staff at the Department of Urology, the Department of Nuclear Medicine and the Department of Clinical Pathology-Cytology Karolinska University Hospital Huddinge for the hard work of recruiting patients, producing SPECT/CT examinations and the histopathological evaluation of MIDOR material respectively. **VINNOVA** financially supported MIDOR project and **Hermes Medical Solutions** provided the software used for the evaluation of MIDOR material.

This research described herein would not have been possible without the support of many to whom **I am deeply grateful**.

First and foremost, Prof. **Rimma Axelsson**, for giving me the opportunity to join her research group. **Rimma,** heartfelt thanks for your trust, motivation, patience and support in all my endeavours over the years. Your everyday example and advice can be followed without hesitation.

My team of co-supervisors and co-authors for the critical comments during the planning of MIDOR project, the evaluation of MIDOR material and the support during publication process: **Maria Holstensson,** Prof. **Torkel B. Brismar, Mattias Karlsson, Eva Hagel, Thomas Papathomas, Stefan Gabrielson, Kiril Trpkov, Georgia Kokaraki, Alexandros Arvanitis, Bela Bozoky, Ove Gustafsson, Na Sun, Alina Bazarova, Wanzhong Wang, Linnea Ekström-Ehn, Franziska Erlmeier, Annette Feuchtinger, Ramin Ghaffarpour,** Prof. **Axel Walch, Anders Svensson, Katharina Brehmer and Georgios Kalarakis.**

Special thanks to my friend, Dr **Thomas Papathomas**. **Thomas,** without you the scientific study n.3 would be impossible.

My friend and mentor Dr **Louiza Loizou**. **Louiza**, many thanks for introducing me to Rimma's research world.

My friend Dr **Stefanos Klironomos** for the final proofreading of this thesis.

All my colleagues in the Abdominal section of Radiology Karolinska University Hospital Huddinge, the Department of Neuroradiology Karolinska and the Department of Nuclear Medicine, Karolinska University Hospital Huddinge. Thank you for **the support**, **the knowled**ge and **the laughs** we share over all these years.

All my teachers and classmates through my life's journey from **Timbaki, Crete** to **Stockholm, Sweden**.

My dear **friends and family** who are named last but certainly not least:

My Swedish crew: Susanne M, Irina S, Ola K, Marie S, Tobias G, Bimma H, Simella K, Nikos V, Giannis P, Giannis D, Georgia K, Foteini L, Dimitris S, Georgios T, Renia P, Mariella T, Villi V, Zacharias M, Pigi D, Evangelos F, Katerina F, Katerina T, Telis D, Gogo P, Gerasimos M, Sokratis O, Maria S, Despoina S, Vaggelis P, Manos S, Marina F

My Greek crew: Eirini K, Maria N, Giannis M, Marianna R, Dimitris C, Giorgos M, Konstantinos T, Eleni Z, Panos K, Sophia G, Aris K, k.Dimitra K, Sarantos S, Nikolas P, Giannis K, Sophia P, Haris M, k.Mairi P, Apostolos T, Nikos K, Themis K, k.Sophia K, k.Antonis K, Georgia T, Pavlos C, Marios M, Giorgos F, Nafsika K, Evi K. Friendship that **goes strong-across countries** and everything that we have gone through during these years. You are **my extended family** and the funniest people I know.

My Cretan crew: giagia Eleni, giagia Klio, pappous Antonis, pappous Giannis, theios Leandros, theia Evangelia, theia Aspasia, theios Nikolaos, uncle Giorgos, uncle Nikos, aunt Anna, aunt Marika, godmother Klio, godfather Giorgos, Giorgos, Iakovos, Mariana, Stella, Andreas L and my ksaderfakia (Eleni, Antonis, Maria, Elias, Lilly, Aphrodite, Tasos, Klio, Mpampis). **My homeland is my childhood.**

Giannis, my wonderful younger brother, my sister-in-law **Sophia** and my niece **Eirini**. The **distance** only makes us **closer** day by day.

My parents **Kostas** and **Rena**. **Mom and Dad, I love you.** You taught me everything I know.

My partner in life **Ioannis Koupidis**. **Giannis**, the fact that this thesis is authored by me and not by Ioannis Koupidis and Antonios Tzortzakakis is a bit unfair. Your practical and emotional support, encouragement and dedication have been invaluable. You are my life's companion, and I am so happy to share this milestone with you.

9 REFERENCES

1. Sánchez-Gastaldo A, Kempf E, González del Alba A, Duran I. Systemic treatment of renal cell cancer: A comprehensive review. Cancer Treat Rev. 2017;60:77–89.

2. Petejova N, Martinek A. Renal cell carcinoma: Review of etiology, pathophysiology and risk factors. Biomed Pap. 2016;160:183–94.

3. Capitanio U, Bensalah K, Bex A, Boorjian SA, Bray F, Coleman J, et al. Epidemiology of Renal Cell Carcinoma [Figure presented]. Eur Urol [Internet]. European Association of Urology; 2019;75:74–84. Available from: https://doi.org/10.1016/j.eururo.2018.08.036

4. Carlo MI, Hakimi AA, Stewart GD, Bratslavsky G, Brugarolas J, Chen YB, et al. Familial Kidney Cancer: Implications of New Syndromes and Molecular Insights. Eur Urol [Internet]. European Association of Urology; 2019;76:754–64. Available from: https://doi.org/10.1016/j.eururo.2019.06.015

5. McIntosh AG, Ristau BT, Ruth K, Jennings R, Ross E, Smaldone MC, et al. Active Surveillance for Localized Renal Masses: Tumor Growth, Delayed Intervention Rates, and >5-yr Clinical Outcomes[Figure presented]. Eur Urol [Internet]. European Association of Urology; 2018;74:157–64. Available from: https://doi.org/10.1016/j.eururo.2018.03.011

6. Znaor A, Lortet-Tieulent J, Laversanne M, Jemal A, Bray F. International variations and trends in renal cell carcinoma incidence and mortality. Eur Urol [Internet]. European Association of Urology; 2015;67:519–30. Available from: http://dx.doi.org/10.1016/j.eururo.2014.10.002

7. Lam ET, Nabi S, Kessler ER, Bernard B, Flaig TW. Renal cell carcinoma: A review of biology and pathophysiology. F1000Research. 2018;7:1–10.

8. Daugherty M, Sedaghatpour D, Shapiro O, Vourganti S, Kutikov A, Bratslavsky G. The metastatic potential of renal tumors: Influence of histologic subtypes on definition of small renal masses, risk stratification, and future active surveillance protocols. Urol Oncol Semin Orig Investig. 2017;35:153.e15-153.e20.

9. Moch H, Cubilla AL, Humphrey PA, Reuter VE, Ulbright TM. The 2016 WHO Classification of Tumours of the Urinary System and Male Genital Organs—Part A: Renal, Penile, and Testicular Tumours. Eur Urol [Internet]. European Association of Urology; 2016;70:93–105. Available from: http://dx.doi.org/10.1016/j.eururo.2016.02.029

10. Udager AM, Mehra R. Morphologic, molecular, and taxonomic evolution of renal cell carcinoma a conceptual perspective with emphasis on updates to the 2016 world health organization classification. Arch Pathol Lab Med. 2016;140:1026–37.

11. Ruiz-Cordero R, Rao P, Li L, Qi Y, Atherton D, Peng B, et al. Hybrid oncocytic/chromophobe renal tumors are molecularly distinct from oncocytoma and chromophobe renal cell carcinoma. Mod Pathol [Internet]. Springer US; 2019;32:1698–707. Available from: http://dx.doi.org/10.1038/s41379-019-0304-y

12. Trpkov K, Hes O. New and emerging renal entities: a perspective post-WHO 2016 classification. Histopathology. 2019;74:31–59.

13. Neves JB, Withington J, Fowler S, Patki P, Barod R, Mumtaz F, et al. Contemporary surgical management of renal oncocytoma: a nation's outcome. BJU Int. 2018;121:893–9.

14. Patel HD, Druskin SC, Rowe SP, Pierorazio PM, Gorin MA, Allaf ME. Surgical histopathology for suspected oncocytoma on renal mass biopsy: a systematic review and meta-analysis. BJU Int. 2017;119:661–6.

15. Woo S, Cho JY. Imaging findings of common benign renal tumors in the era of small renal masses: Differential diagnosis from small renal cell carcinoma – current status and future perspectives. Korean J Radiol. 2015;16:99–113.

16. Amin J, Xu B, Badkhshan S, Creighton TT, Abbotoy D, Murekeyisoni C, et al. Identification and validation of radiographic enhancement for reliable differentiation of CD117(þ) benign renal oncocytoma and chromophobe renal cell carcinoma. Clin Cancer Res. 2018;24:3898–907.

17. Abualjadayel MH, Safdar OY, Banjari MA, El Desoky S, Mokhtar GA, Azhar RA. A Rare Benign Tumor in a 14-Year-Old Girl. Case Reports Nephrol. Hindawi; 2018;2018:1–4.

18. Vogel C, Ziegelmüller B, Ljungberg B, Bensalah K, Bex A, Canfield S, et al. Imaging in Suspected Renal-Cell Carcinoma: Systematic Review. Clin Genitourin Cancer. 2019;17:e345–55.

19. Yu Y, Ma L, Wang Z, Zhang Z. Renal cell carcinoma presenting as a simple renal cyst: A case report. Mol Clin Oncol. 2017;6:550–2.

20. Ljungberg B, Albiges L, Abu-Ghanem Y, Bensalah K, Dabestani S, Montes SFP, et al. European Association of Urology Guidelines on Renal Cell Carcinoma: The 2019 Update. Eur Urol. 2019;75:799–810.

21. Pastore AL, Palleschi G, Silvestri L, Moschese D, Ricci S, Petrozza V, et al. Serum and urine biomarkers for human renal cell carcinoma. Dis Markers. 2015;2015.

22. Falegan OS, Egloff SAA, Zijlstra A, Hyndman ME, Vogel HJ. Urinary metabolomics validates metabolic differentiation between renal cell carcinoma stages and reveals a unique metabolic profile for oncocytomas. Metabolites. 2019;9.

23. Farber NJ, Kim CJ, Modi PK, Hon JD, Sadimin ET, Singer EA. Renal cell carcinoma: The search for a reliable biomarker. Transl Cancer Res. 2017;6:620–32.

24. Kalarakis G, Brehmer K, Svensson A, Axelsson R, Brismar TB, Tzortzakakis A. Combining contrast-enhanced ultrasound, CT perfusion and 99m Tc-Sestamibi SPECT/CT to guide diagnosis in a case of solid renal tumour 1. 2020;

25. Rossi SH, Klatte T, Usher-Smith J, Stewart GD. Epidemiology and screening for renal cancer. World J Urol [Internet]. Springer Berlin Heidelberg; 2018;36:1341–53. Available from: https://doi.org/10.1007/s00345-018-2286-7

26. Vos N, Oyen R. Renal angiomyolipoma: The good, the bad, and the ugly. J Belgian Soc Radiol. 2018;102:1–9.

27. Giambelluca D, Pellegrino S, Midiri M, Salvaggio G. The "central stellate scar" sign in renal oncocytoma. Abdom Radiol [Internet]. Springer US; 2019;44:1942–3. Available from: https://doi.org/10.1007/s00261-019-01899-3

28. Ishigami K, Jones AR, Dahmoush L, Leite L V., Pakalniskis MG, Barloon TJ. Imaging spectrum of renal oncocytomas: a pictorial review with pathologic correlation. Insights Imaging. 2015;6:53–64.

29. Hodgdon T, McInnes MDF, Schieda N, Flood TA, Lamb L, Thornhill RE. Can quantitative CT texture analysis be used to differentiate fat-poor renal angiomyolipoma from renal cell carcinoma on unenhanced CT images? Radiology. 2015;276:787–96.

30. Zhang GMY, Shi B, Xue HD, Ganeshan B, Sun H, Jin ZY. Can quantitative CT texture analysis be used to differentiate subtypes of renal cell carcinoma? Clin Radiol [Internet]. The Royal College of Radiologists; 2019;74:287–94. Available from: https://doi.org/10.1016/j.crad.2018.11.009

31. Li Y, Huang X, Xia Y, Long L. Value of radiomics in differential diagnosis of chromophobe renal cell carcinoma and renal oncocytoma. Abdom Radiol [Internet]. Springer US; 2019;45:3193–201. Available from: https://doi.org/10.1007/s00261-019-02269-9

32. Tordjman M, Mali R, Madelin G, Prabhu V, Kang SK. Diagnostic test accuracy of ADC values for identification of clear cell renal cell carcinoma: systematic review and meta-analysis. Eur Radiol. European Radiology; 2020;30:4023–38.

33. Bertolotto M, Bucci S, Valentino M, Currò F, Sachs C, Cova MA. Contrast-enhanced ultrasound for characterizing renal masses. Eur J Radiol [Internet]. Elsevier; 2018;105:41–8. Available from: https://doi.org/10.1016/j.ejrad.2018.05.015

34. Rossi SH, Prezzi D, Kelly-Morland C, Goh V. Imaging for the diagnosis and response assessment of renal tumours. World J Urol [Internet]. Springer Berlin Heidelberg; 2018;36:1927–42. Available from: https://doi.org/10.1007/s00345-018-2342-3

35. Liu Y. The place of FDG PET/CT in renal cell carcinoma: Value and limitations. Front Oncol. 2016;7:1–7.

36. Lindenberg L, Mena E, Choyke PL, Bouchelouche K. PET imaging in renal cancer. Curr Opin Oncol. 2019;31:216–21.

37. Das CJ. Perfusion computed tomography in renal cell carcinoma. World J Radiol. 2015;7:170.

38. Mazzei FG, Mazzei MA, Squitieri NC, Pozzessere C, Righi L, Cirigliano A, et al. CT perfusion in the characterisation of renal lesions: An added value to multiphasic CT. Biomed Res Int. 2014;2014.

39. Chen C, Liu Q, Hao Q, Xu B, Ma C, Zhang H, et al. Study of 320-slice dynamic volume CT perfusion in different pathologic types of kidney tumor: Preliminary results. PLoS One. 2014;9.

40. Wang Y, Cui L, Zhang J, Zhang L, Zhang J, Zhao X, et al. Baseline perfusion CT parameters as potential biomarkers in predicting long-term prognosis of localized clear cell renal cell carcinoma. Abdom Radiol [Internet]. Springer US; 2019;44:3370–6. Available from: https://doi.org/10.1007/s00261-019-02087-z

41. Reiner CS, Roessle M, Thiesler T, Eberli D, Klotz E, Frauenfelder T, et al. Computed tomography perfusion imaging of renal cell carcinoma: Systematic comparison with histopathological angiogenic and prognostic markers. Invest Radiol. 2013;48:183–91.

42. Chen Y, Zhang J, Dai J, Feng X, Lu H, Zhou C. Angiogenesis of renal cell carcinoma: Perfusion CT findings. Abdom Imaging. 2010;35:622–8.

43. Abdessater M, Kanbar A, Comperat E, Dupont-Athenor A, Alechinsky L, Mouton M, et al. Renal Oncocytoma: An Algorithm for Diagnosis and Management. Urology [Internet]. Elsevier Inc.; 2020; Available from: https://doi.org/10.1016/j.urology.2020.05.047

44. Wilson MP, Katlariwala P, Murad MH, Abele J, McInnes MDF, Low G. Diagnostic accuracy of 99mTc-sestamibi SPECT/CT for detecting renal oncocytomas and other benign renal lesions: a systematic review and meta-analysis. Abdom Radiol [Internet]. Springer US; 2020;45:2532–41. Available from: https://doi.org/10.1007/s00261-020-02469-8

45. Rowe SP, Gorin MA, Solnes LB, Ball MW, Choudhary A, Pierorazio PM, et al. Correlation of 99mTc-sestamibi uptake in renal masses with mitochondrial content and multi-drug resistance pump expression. EJNMMI Res. EJNMMI Research; 2017;7.

46. Gormley TS, Van Every MJ, Moreno AJ. Renal oncocytoma: Preoperative diagnosis using technetium 99m sestamibi imaging. Urology. 1996;48:33–9.

47. Rowe SP, Gorin MA, Gordetsky J, Ball MW, Pierorazio PM, Higuchi T, et al. Initial experience using 99mTc-MIBI SPECT/CT for the differentiation of oncocytoma from renal cell carcinoma. Clin Nucl Med. 2015;40:309–13.

48. Gorin MA, Rowe SP, Baras AS, Solnes LB, Ball MW, Pierorazio PM, et al. Prospective Evaluation of 99mTc-sestamibi SPECT/CT for the Diagnosis of Renal Oncocytomas and Hybrid Oncocytic/Chromophobe Tumors. Eur Urol [Internet]. European Association of Urology; 2016;69:413–6. Available from: http://dx.doi.org/10.1016/j.eururo.2015.08.056

49. Ljungberg M, Pretorius PH. SPECT/CT: an update on technological developments and clinical applications. Br J Radiol. 2018;91:20160402.

50. Dickson J, Ross J, Vöö S. Quantitative SPECT: the time is now. EJNMMI Phys. EJNMMI Physics; 2019;6:1–7.

51. Montironi R, Gasparrini S, Cimadamore A, Mazzucchelli R, Massari F, Cheng L, et al. Variants and Variations in Epithelial Renal Cell Tumors in Adults: The Pathologist's Point of View. Eur Urol Suppl [Internet]. European Association of Urology; 2017;16:232–40. Available from: http://dx.doi.org/10.1016/j.eursup.2017.08.008

52. Wobker SE, Williamson SR. Modern Pathologic Diagnosis of Renal Oncocytoma. J Kidney Cancer VHL. 2017;4:1–12.

53. Delahunt B, Eble JN, Egevad L, Samaratunga H. Grading of renal cell carcinoma. Histopathology. 2019;74:4–17.

54. Shen SS, Ro JY. Histologic diagnosis of renal mass biopsy. Arch Pathol Lab Med. 2019;143:705–10.

55. Buck A, Ly A, Balluff B, Sun N, Gorzolka K, Feuchtinger A, et al. High-resolution MALDI-FT-ICR MS imaging for the analysis of metabolites from formalin-fixed, paraffin-embedded clinical tissue samples. J Pathol. 2015;237:123–32.

56. Andeen NK, Qu X, Antic T, Tykodi SS, Fang M, Tretiakova MS. Clinical utility of chromosome genomic array testing for unclassified and advanced-stage renal cell carcinomas.

Arch Pathol Lab Med. 2019;143:494–504.

57. Erlmeier F, Feuchtinger A, Borgmann D, Rudelius M, Autenrieth M, Walch AK, et al. Supremacy of modern morphometry in typing renal oncocytoma and malignant look-alikes. Histochem Cell Biol. Springer Berlin Heidelberg; 2015;144:147–56.

58. Jewett MAS, Mattar K, Basiuk J, Morash CG, Pautler SE, Siemens DR, et al. Active surveillance of small renal masses: Progression patterns of early stage kidney cancer. Eur Urol. 2011;60:39–44.

59. Bianchi FM, Bianchi L, Chessa F, Barbaresi U, Casablanca C, Mottaran A, et al. How to select patients with small renal mass for ablation or partial nephrectomy? the impact of histologic variant and tumor's size. Eur Urol Open Sci [Internet]. Elsevier B.V.; 2020;20:S119. Available from: http://dx.doi.org/10.1016/S2666-1683(20)35509-9

60. Renner A, Samtani SR, Marín A, Burotto M. Is Cytoreductive Nephrectomy Still a Standard of Care in Metastatic Renal Cell Carcinoma? J Kidney Cancer VHL. 2019;6:1–7.

61. Tzortzakakis A, Gustafsson O, Karlsson M, Ekström-Ehn L, Ghaffarpour R, Axelsson R. Visual evaluation and differentiation of renal oncocytomas from renal cell carcinomas by means of 99mTc-sestamibi SPECT/CT. EJNMMI Res. EJNMMI Research; 2017;7.

62. Tzortzakakis A, Holstensson M, Hagel E, Karlsson M, Axelsson R. Intra- and Interobserver Agreement of SUV SPECT Quantitative SPECT/CT Processing Software, Applied in Clinical Settings for Patients with Solid Renal Tumors. J Nucl Med Technol. 2019;47:258–62.

63. Ly A, Buck A, Balluff B, Sun N, Gorzolka K, Feuchtinger A, et al. High-mass-resolution MALDI mass spectrometry imaging of metabolites from formalin-fixed paraffin-embedded tissue. Nat Protoc. Nature Publishing Group; 2016;11:1428–43.

64. Papathomas T, Tzortzakakis A, Sun N, Erlmeier F, Bozoky B, Kokaraki G, et al. In Situ Metabolomics Expands the Spectrum of Renal Tumours Positive on 99m Tc-sestamibi Single Photon Emission Computed Tomography / Computed Tomography Examination. Eur Urol Open Sci [Internet]. European Association of Urology.; 2020;22:88–96. Available from: https://doi.org/10.1016/j.euros.2020.11.001

65. Trpkov K, Williamson SR, Gao Y, Martinek P, Cheng L, Sangoi AR, et al. Low-grade oncocytic tumour of kidney (CD117-negative, cytokeratin 7-positive): a distinct entity? Histopathology. 2019;75:174–84.

66. Petersson F, Gatalica Z, Grossmann P, Perez Montiel MD, Alvarado Cabrero I, Bulimbasic S, et al. Sporadic hybrid oncocytic/chromophobe tumor of the kidney: A clinicopathologic, histomorphologic, immunohistochemical, ultrastructural, and molecular cytogenetic study of 14 cases. Virchows Arch. 2010;456:355–65.

67. Asi T, Tuncali MÇ, Tuncel M, Alkanat NEİ, Hazir B, Kösemehmetoğlu K, et al. The role of Tc-99m MIBI scintigraphy in clinical T1 renal mass assessment: Does it have a real benefit? Urol Oncol Semin Orig Investig. 2020;000.

68. Zhu H, Yang B, Dong A, Ye H, Cheng C, Pan G, et al. Dual-Phase 99mTc-MIBI SPECT/CT in the characterization of enhancing solid renal tumors: A single-institution study of 147 Cases. Clin Nucl Med. 2020;45:765–70.

69. Health L, Centre S. CUAJ – Original Research Sistani et al MIBI SPECT-CT for evaluation

and risk stratification of RCC The value of. 2020;

70. Su ZT, Patel HD, Huang MM, Meyer AR, Pavlovich CP, Pierorazio PM, et al. Cost-effectiveness Analysis of 99mTc-sestamibi SPECT/CT to Guide Management of Small Renal Masses. Eur Urol Focus [Internet]. European Association of Urology; 2020;1–8. Available from: https://doi.org/10.1016/j.euf.2020.02.010